Article

Cell

The Neuropeptide Tac2 Controls a Distributed Brain State Induced by Chronic Social Isolation Stress

Graphical Abstract

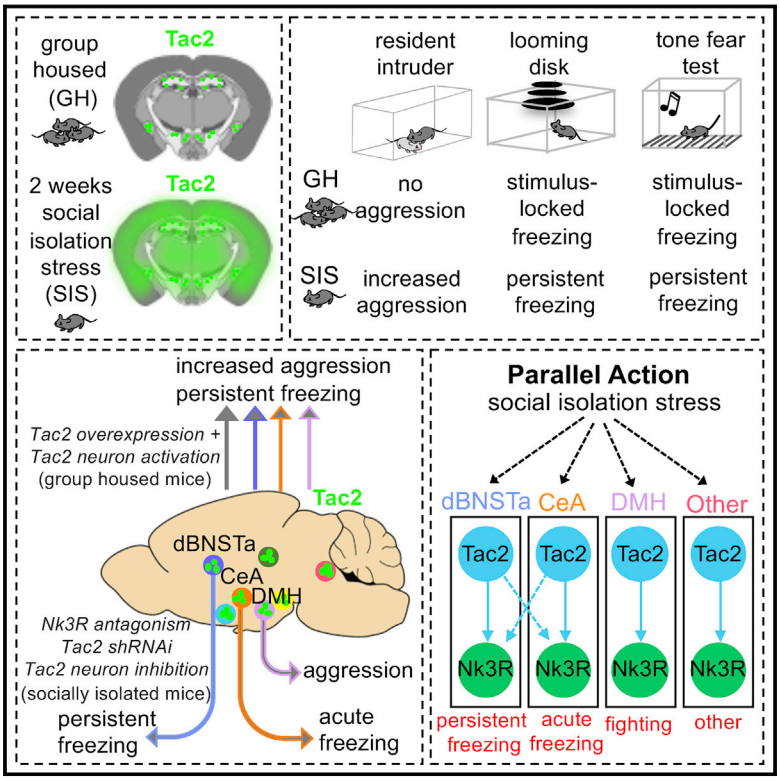

Highlights

- Chronic social isolation stress (SIS) causes a pervasive change in brain state
- SIS broadly upregulates expression of Tac2/NkB in multiple brain regions
- Tac2 upregulation is necessary and sufficient for behavioral influences of SIS
- NkB acts locally in different brain areas to orchestrate behavioral effects of SIS

Authors

Moriel Zelikowsky, May Hui, Tomomi Karigo, ..., Viviana Gradinaru, Benjamin E. Deverman, David J. Anderson

Correspondence

moriel@caltech.edu (M.Z.), wuwei@caltech.edu (D.J.A.)

In Brief

The Tac2 neuropeptide system orchestrates the complex behavioral effects of chronic social isolation stress by acting locally in multiple brain regions, suggesting the therapeutic potential of Nk3R antagonists for managing behavioral changes upon prolonged social isolation.

Zelikowsky et al., 2018, Cell *173*, 1265–1279
May 17, 2018
https://doi.org/10.1016/j.cell.2018.03.037

CellPress

Cell

The Neuropeptide Tac2 Controls a Distributed Brain State Induced by Chronic Social Isolation Stress

Moriel Zelikowsky,[1,*] May Hui,[1] Tomomi Karigo,[1] Andrea Choe,[1] Bin Yang,[1] Mario R. Blanco,[1] Keith Beadle,[1] Viviana Gradinaru,[1] Benjamin E. Deverman,[1,4] and David J. Anderson[1,2,3,5,*]

[1]Division of Biology and Biological Engineering 156-29, California Institute of Technology, Pasadena, CA 91125, USA

[2]Howard Hughes Medical Institute, California Institute of Technology, Pasadena, CA 91125, USA

[3]Tianqiao and Chrissy Chen Institute for Neuroscience, California Institute of Technology, Pasadena, CA 91125, USA

[4]Present address: The Stanley Center for Psychiatric Research at the Broad Institute of MIT and Harvard, 75 Ames Street, Cambridge, MA 02142, USA

[5]Lead Contact

*Correspondence: moriel@caltech.edu (M.Z.), wuwei@caltech.edu (D.J.A.)

https://doi.org/10.1016/j.cell.2018.03.037

SUMMARY

Chronic social isolation causes severe psychological effects in humans, but their neural bases remain poorly understood. 2 weeks (but not 24 hr) of social isolation stress (SIS) caused multiple behavioral changes in mice and induced brain-wide upregulation of the neuropeptide tachykinin 2 (Tac2)/neurokinin B (NkB). Systemic administration of an Nk3R antagonist prevented virtually all of the behavioral effects of chronic SIS. Conversely, enhancing NkB expression and release phenocopied SIS in group-housed mice, promoting aggression and converting stimulus-locked defensive behaviors to persistent responses. Multiplexed analysis of Tac2/NkB function in multiple brain areas revealed dissociable, region-specific requirements for both the peptide and its receptor in different SIS-induced behavioral changes. Thus, Tac2 coordinates a pleiotropic brain state caused by SIS via a distributed mode of action. These data reveal the profound effects of prolonged social isolation on brain chemistry and function and suggest potential new therapeutic applications for Nk3R antagonists.

INTRODUCTION

Internal states of arousal, motivation, and emotion exert a major influence on how the brain processes sensory information to control behavior (Berridge, 2004; Bargmann, 2012; LeDoux, 2012; Anderson and Adolphs, 2014; Anderson, 2016). An important class of internal states is that produced by exposure to psychogenic stressors (McEwen et al., 2015). Chronic stress in particular has profound, long-lasting effects on both physical and mental health (Selye, 1936; House et al., 1988; Sapolsky, 1996; Cacioppo and Hawkley, 2009; Kessler et al., 2009; Holt-Lunstad et al., 2010, 2015; Cacioppo et al., 2014). However, most animal models of chronic stress entail repeated administration of acute stressors and hence contain within them a reprieve from the stressor (Katz et al., 1981). Thus, although the stress is repeatedly administered, it is intermittent.

Chronic social isolation stress (SIS) provides one of the few paradigms in which a stressor can be applied continuously for extended periods (days or weeks) (Hilakivi et al., 1989; Weiss et al., 2004). SIS is widespread in humans and has detrimental effects on health (House et al., 1988). However, its neurobiological basis remains poorly understood. For example, there is conflicting evidence on whether or not prolonged SIS chronically activates the HPA axis (Hawkley et al., 2012; Cacioppo et al., 2015). A recent study implicated dorsal raphe dopaminergic neurons in mediating effects of relatively brief (24 hr) social isolation in mice (Matthews et al., 2016), but a subsequent study described a broader role for these neurons in promoting arousal (Cho et al., 2017).

Neuropeptides, most notably CRH, have been implicated in mediating stress responses in a variety of systems (reviewed in Kormos and Gaszner [2013]; Witkin et al. [2014]; Kash et al. [2015]; Chen [2016]), but the logic underlying their actions is not yet clear (Figures 1A–1D). Guided by our previous studies of aggression in *Drosophila* (Wang et al., 2008; Asahina et al., 2014), we have investigated a potential role for tachykinins in mediating SIS-induced aggression in mice (Maggio, 1988). Studies of the neuropeptide tachykinin 2 (Tac2)/neurokinin B (NkB) in the central amygdala have implicated the peptide in fear memory consolidation (Andero et al., 2014, 2016), suggesting a role in fear learning and expression. Here, we report a broader and unanticipated role for Tac2/NkB as an important peptide mediator of the effects of chronic SIS. Tac2/NkB is dramatically upregulated by SIS throughout the brain and coordinates a pervasive change in brain state, affecting not only aggression but also many other behaviors via distributed local actions in multiple brain regions.

RESULTS

Chronic SIS Produces Widespread Effects on Multiple Defensive Behaviors

Prolonged SIS is known to promote multiple behavioral effects, including increased aggression and persistent responses to

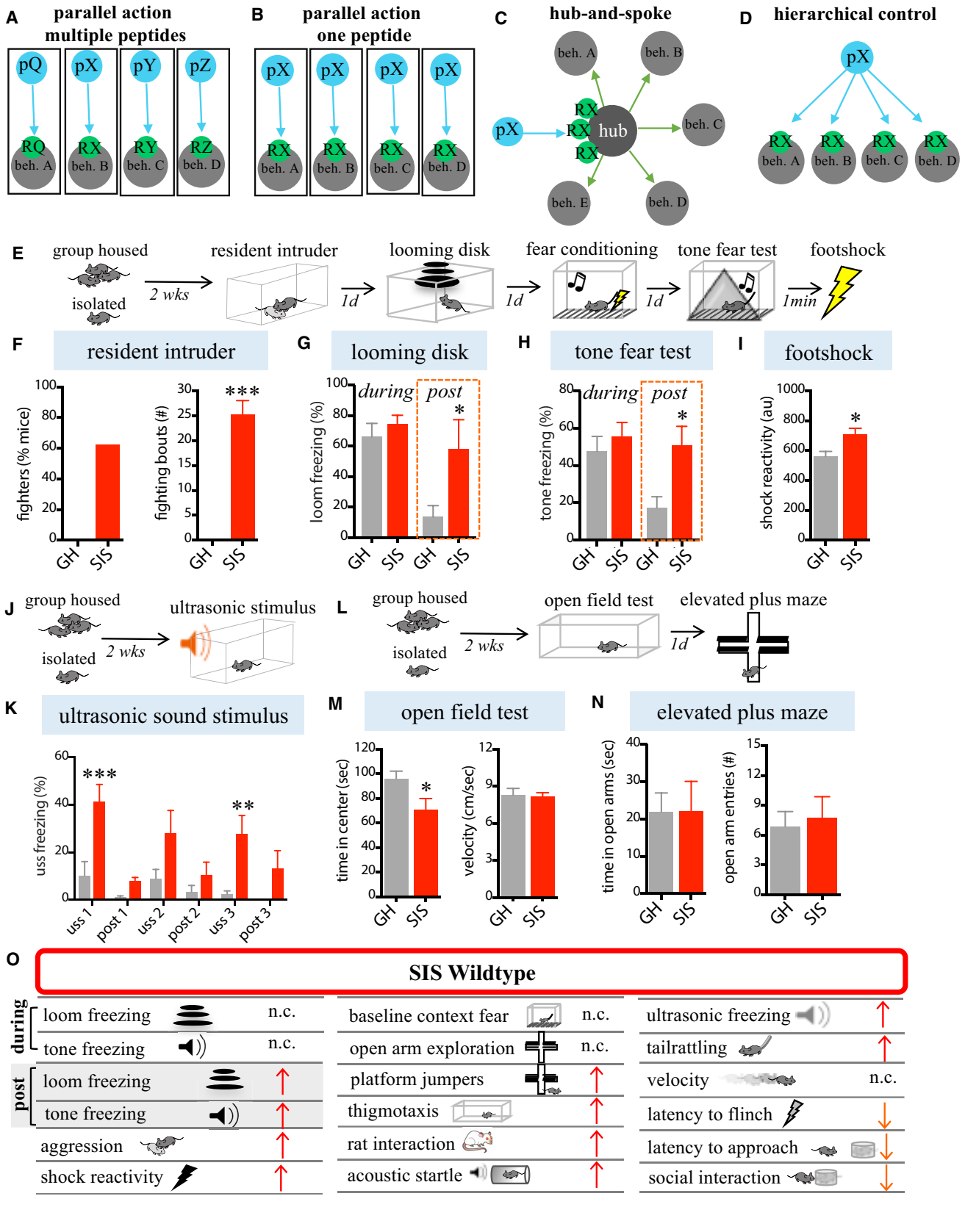

(legend on next page)

threats, in both humans and animal models (Wiberg and Grice, 1963; Valzelli, 1969, 1973; Weiss et al., 2004; Matsumoto et al., 2005; Arrigo and Bullock, 2008; An et al., 2017). As an initial step, therefore, we examined the effects of 2 weeks of SIS in wild-type C57Bl6/N mice using multiple behavioral assays: aggression in the resident-intruder (RI) assay (Thurmond, 1975), innate freezing to an overhead looming disk (LD) (Yilmaz and Meister, 2013), learned freezing to a conditioned tone (2.8 kHz) (Fanselow, 1980), and reactivity to a footshock (0.7mA) (Figures 1E–1I and S1B–S1D). SIS produced a robust increase in offensive aggression toward a submissive intruder, compared to non-aggressive group-housed controls (Figure 1F), confirming previous studies (Valzelli, 1969; Matsumoto et al., 2005; Toth et al., 2011). It also caused persistent freezing to both the LD and tone (Figures 1G and 1H, "post," red bars), in contrast to GH controls where freezing terminated with stimulus offset. However, the magnitude of freezing to both the overhead LD and the conditioned tone was unaffected by SIS (Figures 1G and 1H, "during"), as was the rate and asymptotic value of conditioned fear acquisition (Figure S1A). SIS mice also showed significantly enhanced reactivity to a footshock (Figure 1I), increased freezing to a threatening ultrasonic stimulus (USS) (Mongeau et al., 2003) (Figures 1J and 1K), increased tail rattling to the LD (Figure S1E), increased sensitivity to sub-threshold acoustic startle stimuli (Figure S1I), and a decreased latency to flinch to a mild footshock (Figure S1H).

SIS mice were also tested for anxiety-like behavior in the open-field test (OFT) and the elevated plus maze (EPM) (Figures 1L–1N and S1F). They showed a modest but significant reduction in time spent in the center of the OFT arena, without a change in velocity (Figure 1M), but were no different from GH mice on the EPM test (Figure 1N). However, SIS mice showed an increased propensity to jump off the EPM platform (Figure S1F). Lastly, SIS mice spent less time interacting with a novel mouse in a social interaction assay (although their latency to initially approach the mouse was reduced; Figure S1J) but more time closer to a predator (rat) (Figure S1G). Collectively, these findings demonstrate that SIS alters behavioral responses to a variety of stimuli (summarized in Figure 1O). This profile appears different from anxiety (Blanchard et al., 2003; Bourin et al., 2007), consistent with earlier studies in mice (Hilakivi et al., 1989). Importantly, when we isolated mice for just 24 hr, we failed to detect any of the behavioral alterations we observed following 2 weeks of SIS (Figures S3A–S3E), distinguishing this paradigm from the effects of short-term isolation studied previously (Matthews et al., 2016).

Chronic SIS Causes Widespread Upregulation of *Tac2* Transcription

In *Drosophila*, an unbiased screen of peptidergic neurons identified DTK (*Drosophila* tachykinin)-expressing neurons and the DTK peptide as required for social isolation-induced aggression (Asahina et al., 2014). To determine whether this function might be conserved, we investigated the role of tachykinins in SIS. In rodents, the tachykinin gene family comprises *Tac1* and *Tac2* (Maggio, 1988). *Tac1* encodes the peptides substance P (SP), as well as neurokinin A (NkA); *Tac2* encodes neurokinin B (NkB). These peptides bind with the highest affinities to the G-protein-coupled Nk1, Nk2, and Nk3 receptors, respectively (Figure 2A) (Ebner et al., 2009). *Tac1* and *Tac2* are expressed in a variety of brain regions implicated in emotion and social behavior (Figure 2B) (Culman and Unger, 1995).

To determine whether *Tac* gene expression is influenced by SIS, we crossed *Tac2-IRES-Cre* or *Tac1-IRES-Cre* knockin mice (Tasic et al., 2016) to a Cre-reporter mouse (line Ai6) expressing zsGreen (Madisen et al., 2010). Double-heterozygous mice were socially isolated for 2 weeks or group housed prior to sacrifice. Strikingly, freshly dissected brains from isolated *Tac2-Cre; Ai6* (but not *Tac1-Cre; Ai6*) mice exhibited enhanced cortical reporter expression that could be detected by the naked eye under ambient lighting (Figure S2A). Histology confirmed a widespread increase in zsGreen expression, in both males (Figures 2C and S2B) and females (Figure S2C). Upregulation was evident in the anterior dorsal bed nucleus of the *stria terminalis* (dBNSTa), central nucleus of the amygdala (CeA), dorsomedial hypothalamus (DMH), and the anterior cingulate cortex (ACC) (Figures S2A and S2B). Cell-specific markers indicated that most zsGreen expression occurred in neuronal cells (Figure S2D). Increased zsGreen expression was also detected in peripheral endocrine tissues, such as the pancreas, testes, and submandibular gland (data not shown).

Similar results were obtained using a different Cre reporter mouse, Ai14 (Madisen et al., 2010) expressing tdTomato (Figure S2E), indicating that the induction was not a peculiarity of the Ai6 line. Importantly, no such change was observed in SIS *Tac1-Cre; Ai6* mice (Figures 2D and S2A). These data suggest

Figure 1. Prolonged SIS Alters Behavior

(A–D) Alternative models for peptidergic control of an internal state influencing multiple behaviors controlled by different brain regions (gray circles, beh. A, beh. B, etc.). Control could be achieved by multiple (A) or a single (B–D) neuropeptide (pQ, pX, etc.) directly acting on multiple regions (A, B, and D) expressing receptors (RX, RY, etc.) for the peptides or on a single peptide-responsive "hub" region (C). In (B) the same peptide (pX) is expressed in different regions (blue circles) that control different behaviors in different peptide-responsive regions (gray circles).

(E–N) A comparison between wild-type (WT) group-housed (GH) control mice and isolated (SIS) mice (n = 8 mice/condition) in the assays indicated (E, J, and L, schematics). (F) Aggression (resident-intruder test). (G and H) Freezing responses during ("during") or immediately after ("post") presentations of an overhead looming disk (G) or conditioned tone (H). (I) Reactivity to footshock following tone test. (K) Freezing to a 17–20 kHz ultrasonic sound stimulus (USS). (M and N) Anxiety assays: open field test (OFT) (M) and elevated plus maze (EPM) test (N).

(O) Summary of results. Red up-pointing arrows indicate isolation-induced increases in behavior; orange down-pointing arrows indicate isolation-reduced behavioral responding. n.c., no change.

In this and in all subsequent figures, data are represented as mean ± SEM. *$p < 0.05$, **$p < 0.01$, ***$p < 0.001$. Pairwise contrasts were tested and corrections for multiple comparisons were applied for post hoc comparisons; bars without asterisks did not reach significance ($p > 0.05$). ANOVA's, *F* values, *t* values, and additional statistical information for this and subsequent figures can be found in Table S1.

See also Figure S1.

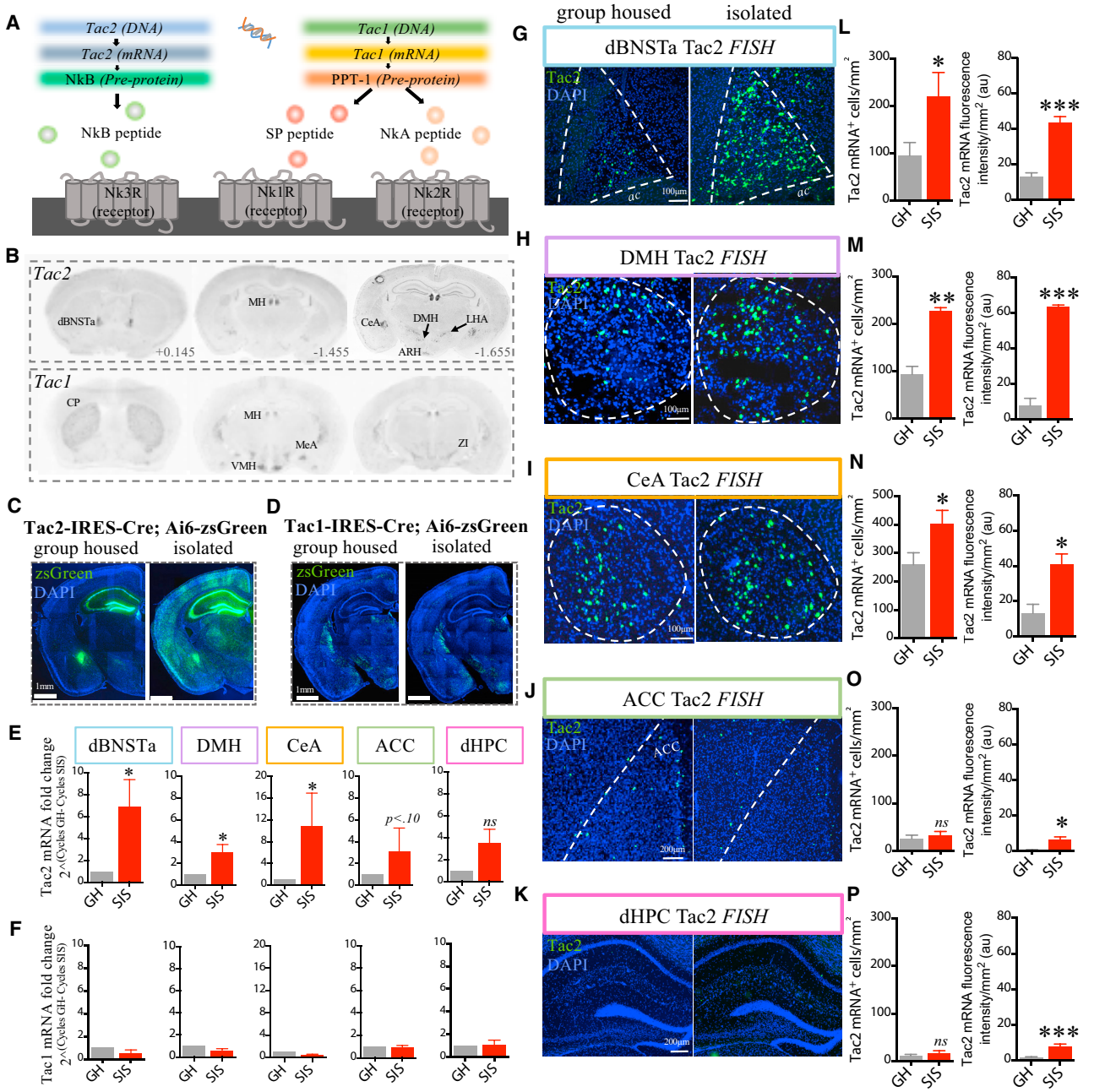

Figure 2. SIS Causes an Increase in Tac2 Expression

(A) Illustration summarizing tachykinin ligand-receptor specificities.

(B) Tac2 (top panels) and Tac1 (bottom panels) mRNA expression (coronal sections) revealed by *in situ* hybridization (ISH) (data from Mouse Brain Atlas, Allen Institute of Brain Science; Tac2, Exp. 72339556; Tac1, Exp.1038). Abbreviations: dBNSTa, antero-dorsal bed nucleus of the *stria terminalis*; MH, medial *habenula*; CeA, central amygdala; DMH, dorsomedial hypothalamus; ARH, arcuate nucleus; LHA, lateral hypothalamus; CP, caudate putamen; MeA, medial amygdala; VMH, ventral medial hypothalamus; and ZI, zona incerta.

(C and D) Coronal sections of expression of zsGreen in GH versus 2-week-isolated Tac2-IRES-Cre (C) or Tac1-IRES-Cre (D) mice crossed to Ai6 (zsGreen) Cre reporter mice.

(E and F) Quantification of Tac2 (E) or Tac1 (F) mRNAs by qRT-PCR in the indicated regions hand-dissected from the brains of GH or SIS mice (n = 4 mice/condition).

(G–K) Tac2 mRNA detected by FISH in GH or SIS mice in the indicated regions (n = 3–4 mice/condition, 1–4 sections/region/mouse); representative sections from dBNST (G), DMH (H), CeA (I), ACC (J), and HPC (K) are shown. Dashed lines indicate regions of interest (ROIs) used for quantification.

(legend continued on next page)

that the induction of zsGreen observed in SIS mice is specific to the *Tac2*^{Cre} allele and is not a non-specific effect of SIS to increase Cre-mediated recombination at the *Rosa-26* locus or a peculiarity of the zsGreen reporter.

To confirm that SIS upregulated endogenous *Tac2* expression, we quantified Tac2 mRNA in selected brain regions using qRT-PCR and RNA fluorescent *in situ* hybridization (FISH). qRT-PCR indicated that SIS caused a large (~3- to 8-fold) and significant increase in Tac2 mRNA levels in the dBNSTa, DMH, and CeA, with trends to an increase in the ACC and dorsal hippocampus (dHPC) (Figure 2E). An increase in NkB protein expression was also observed in these regions by immunostaining (Figure S2I). A time course revealed a gradual increase in Tac2 mRNA from 30 min to 2 weeks of SIS (Figure S2F). No increase in Tac1 mRNA was observed following SIS (Figures 2F and S2G).

Endogenous Tac2 mRNA upregulation was also observed by FISH in in dBNSTa, CeA, and DMH (Figures 2G–2P). Upregulation in CeA was significant in both its medial and lateral subdivisions (Kim et al., 2017). The fold increase in fluorescence intensity per square millimeter was much greater than the fold increase in the number of Tac2 mRNA$^+$ cells (Figures 2L–2P). In contrast, the Cre reporter transgene, which integrates and amplifies changes in expression, yielded a larger fold increase in the number of positive cells (Figure S2B). This difference was particularly evident in the ACC or dHPC (Figures 2J, 2K, 2O, 2P, and S2B), suggesting amplification of induction by the Cre reporter. Despite these quantitative differences, the mRNA data confirm that SIS upregulates endogenous Tac2 expression in multiple brain regions.

Acute Systemic Antagonism of Nk3Rs Attenuates the Effects of SIS

To investigate a causal role for NkB in mediating behavioral effects of SIS, we systemically administered osanetant (Figure 3A) (Emonds-Alt et al., 1995), a specific Nk3R antagonist that crosses the blood-brain barrier (Spooren et al., 2005). Osanetant delivered after SIS, but 20 min prior to each test, strongly reduced aggression enhanced by SIS (Figure 3B), but not by sexual experience (Remedios et al., 2017) (Figures S3J and S3K). It also attenuated persistent freezing to both the LD and the fear-conditioned tone (Figures 3C and 3D, "post," green bars), but not acute freezing during stimulus presentation. Osanetant also attenuated other SIS-induced behaviors including increased shock reactivity (Figure 3E), increased tail rattling (Figure S3G), decreased social interaction (Figure S3H) and enhanced responding in the acoustic startle assay (Figure S3I). Thus, systemic antagonism of Nk3Rs blocked virtually all of the measured behavioral effects of chronic SIS, while leaving non-SIS altered behaviors intact (Figure S3K). Notably, osanetant also blocked persistent freezing to the LD caused by prior footshock (Figures S3L and S3M), suggesting involvement of NkB in responses to other stressors.

Chronic Systemic Antagonism of Nk3Rs during SIS Has a Protective Effect

To investigate whether Tac2 signaling is required during SIS, mice were administered osanetant daily in their home cage during the 2-week isolation period, but were then tested off-drug. To control for carryover of the drug from the last home-cage administration into the testing period (24 hr later), an additional group of SIS mice was given a single home-cage administration of osanetant 24 hr prior to testing (Figure 3F).

Treatment with daily osanetant prevented SIS-enhanced aggression (Figure 3G), persistent freezing to the LD (Figure 3H), and persistent freezing to the fear conditioned tone (Figure 3I). The SIS-induced increase in shock reactivity was reduced, but not significantly (Figures 3J and 3K). Strikingly, mice that had been treated with osanetant during SIS could be returned to housing with their pre-isolation cagemates without any subsequent fighting observed, in contrast to control SIS mice which vigorously attacked their cagemates when reintroduced to the group (data not shown).

Nk3Rs Act in Different Brain Regions to Mediate the Effects of SIS on Different Behaviors

Next, we asked where in the brain NkB signaling is required to mediate the behavioral effects of SIS. The dBNSTa, DMH, and CeA exhibited strong induction of Tac2 by SIS (Figure 2), and also contain cells expressing Nk3Rs (Figure S4A). Since Tac2$^+$ neurons in CeA and dBNSTa project to multiple distal targets (Figures S4B–S4D; Table S2), as a first step, we pharmacologically inhibited Nk3Rs locally in these Tac2-expressing regions. SIS mice received bilateral microinfusions of osanetant into a given region 20 min prior to each behavioral test (Figure 4A). We selected four assays—the RI assay, LD, fear conditioning, and shock reactivity—that exhibit robust SIS-induced changes and could be performed sequentially within the same animals without affecting each other (as indicated by initial experiments in which LD and fear conditioning were performed independently) (Figures S1C and S1D).

Local infusion of osanetant in dBNSTa selectively inhibited persistent, but not acute, freezing to both the LD and the conditioned tone (Figures 4C and 4D), but had no effect on aggression (Figure 4B) or shock reactivity (Figure S4F). By contrast, osanetant microinfused into the DMH abolished aggression (Figure 4E), but had no effect on persistent responses to the LD (Figure 4F) or the conditioned tone (Figure 4G), or on footshock reactivity (Figure S4G). (However, DMH-infused mice showed an increase in the latency to first orient and freeze to the LD; Figure S4E). Lastly, osanetant infusion into the CeA reduced acute (and thereby persistent) freezing to the innate and conditioned threatening stimuli, as well as reactivity to the footshock (Figures 4H–4K and S4H), but not aggression. Infusion of osanetant into the ACC or striatum failed to yield significant effects on SIS-induced persistent freezing to the LD (Figures S4I and S4J).

(L–P) Left, average number of Tac2 mRNA$^+$ cells/mm^2 in ROIs; right, average fluorescence intensity/mm^2 in the regions shown in dBNST (L), DMH (M), CeA (N), ACC (O), and HPC (P), respectively. Fold increases in Tac2 mRNA fluorescence intensity are greater than increases in cell number, indicating an increase in expression level per cell.
See also Figure S2.

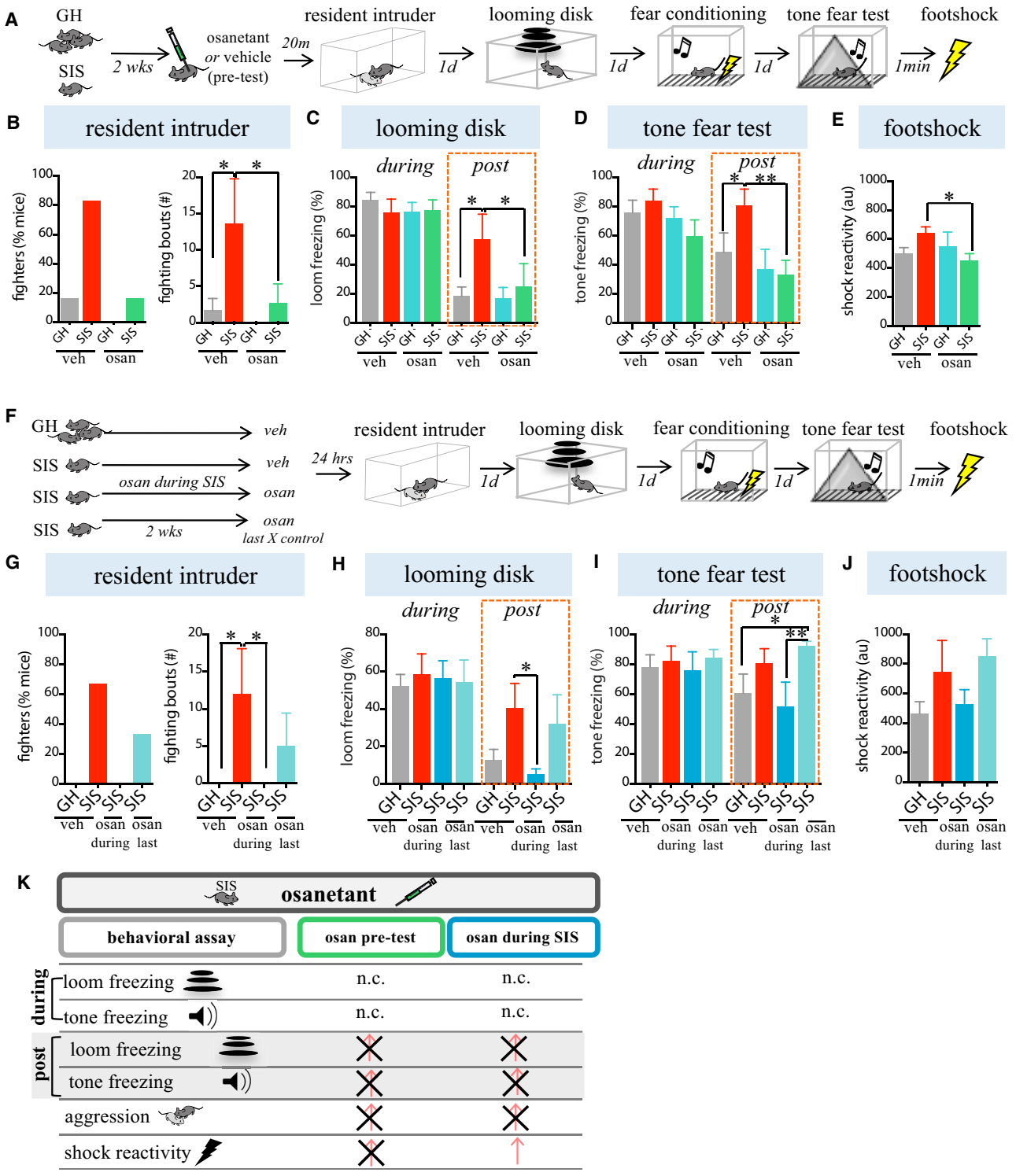

Figure 3. Systemic Nk3R Antagonism Attenuates Effects of SIS

(A) Experimental protocol. Following isolation, SIS or GH mice were injected (i.p.) with osanetant or vehicle and tested for the indicated behaviors (n = 6 mice/condition).

(B–E) Osanetant blocked SIS-induced aggression (B), post-loom freezing (C), and post-tone freezing (D) and increased shock reactivity (E).

(F) Experiment to test whether osanetant delivered daily during SIS can protect against its behavioral effects. "osan last" indicates an additional control group given just the last dose of osan 24 hr before testing to control for drug carryover (n = 6/condition).

(legend continued on next page)

Region-Specific Chemogenetic Silencing of Tac2$^+$ Neurons Blocks Distinct Behavioral Responses to SIS

To determine whether Tac2 upregulation in dBNSTa, DMH and CeA reflected a requirement for NkB release in these structures, we first asked whether the activity of Tac2$^+$ neurons in these regions was required for the effects of SIS. Tac2/c-*fos* dFISH experiments revealed a significant induction of c-*fos* in Tac2$^+$ cells in dBNSTa and CeA following exposure to the LD or conditioned tone, but not during aggression. Conversely, Tac2$^+$ cells in DMH were activated during aggression, but not during threat exposure (Figures S5A–S5D).

To determine whether silencing Tac2$^+$ cells could prevent the effects of SIS, Tac2-IRES-Cre mice were bilaterally injected in dBNSTa, CeA, or DMH with a Cre-dependent adeno-associated virus (AAV) encoding hM4DREADD (AAV2-DIO-hM4D-mCherry) (Conklin et al., 2008). Following 3 weeks to allow viral expression (Figure S5E) and 2 weeks of SIS, mice were tested for SIS-induced behavioral changes 20 min after injection of clozapine-N-oxide (CNO) or vehicle (Figure 5A).

Chemogenetic silencing of Tac2$^+$ cells in dBNSTa, DMH, and CeA essentially phenocopied the effect of local osanetant infusions. In dBNSTa, persistent freezing responses were selectively attenuated (Figures 5B–5D, *post*), while in DMH aggression was inhibited (Figures 5E–5G), and in CeA acute freezing and shock reactivity were suppressed (Figures 5H–5K and S5H). No effects of CNO were observed in control mice subjected to the same series of behavioral assays (Figures 5SI–5SN), excluding off-target effects (Gomez et al., 2017). Thus the activity of Tac2$^+$ neurons, like Nk3R function, is differentially required in different brain regions for different behavioral effects of SIS.

Tac2 Synthesis Is Differentially Required in dBNSTa, CeA, and DMH

We asked next whether Tac2 synthesis was required in each of the three brain regions studied, via targeted small hairpin RNA interference (shRNAi)-mediated knockdown of Tac2. Mice were injected stereotaxically in dBNSTa, DMH, or CeA with adeno-associated viruses (AAVs) expressing small hairpin RNAs (shRNAs), together with a CMV promoter-driven zsGreen fluorescent reporter (AAV5-H1-shRNA-CMV-zsGreen). Two shRNAs (shRNA-1 and shRNA-2) proved effective as determined by FISH and qRT-PCR, with shRNA-2 yielding the strongest reductions in Tac2 mRNA (Figures S6E–S6G). Control mice were injected with an AAV encoding an shRNA targeted to the *luciferase* gene. Injections were histologically verified by zsGreen fluorescence. The number of zsGreen$^+$ neurons was not significantly different between animals injected with control versus experimental shRNAs, suggesting that the reduction in the number of Tac2 mRNA$^+$ cells was not due to cell death (Figure S6D).

In DMH both shRNAs strongly attenuated SIS-induced aggression, but had no significant effect on freezing (Figures 6E–6G), similar to the effect of Tac2$^+$ neuron silencing or local infusion of osanetant in this region (Figures 4E–4G and Figures 5E–5G). Conversely, in the dBNSTa shRNA-1 strongly reduced persistent freezing to both the LD and the conditioned tone (Figures 6C and 6D, red bars, "post"), but had no effect on acute freezing to the threatening stimuli (Figures 6C and 6D, red bars, "during"), or on SIS-induced aggression (Figure 6B). Notably, unlike the case with Tac2$^+$ neuron silencing and local osanetant infusion, the stronger shRNA-2 expressed in dBNSTa significantly reduced acute as well as persistent freezing to both the LD and conditioned tone (Figures 6C, 6D, 6I, and 6J, "during," orange bars). In CeA, Tac2 shRNA2 reduced acute freezing during and after stimulus presentation (Figure 6I), but had no effect on aggression (Figure 6H). The fact that local inhibition of Tac2 synthesis or of Tac2$^+$ neuronal activity yielded similar behavioral effects (Figures 5K and 6K) supports a requirement for Tac2 release in the effects of SIS.

Enhancement of Tac2 Expression and Tac2$^+$ Neuronal Activity Mimics the Effects of SIS

The foregoing findings indicate that Tac2 is required for the collective behavioral effects of SIS. However, because there is baseline Tac2 expression in these regions in GH mice (Figures 2B and 2E), these data do not distinguish whether Tac2 upregulation per se mediates the effects of SIS, or whether Tac2 is simply permissive. Therefore, we asked whether increasing the level and/or release of Tac2 was sufficient to mimic any of the behavioral effects of SIS, in group-housed animals.

To do this, we injected intravenously into GH Tac2-IRES-Cre (gene-conserving) driver mice (Figure S7) Cre-dependent vectors encoding the DREADD neuronal activator hM3D; a Tac2 cDNA or control mCherry using the AAV serotype PHP.B, which crosses the blood-brain barrier (Deverman et al., 2016). Following 3 weeks to allow for viral expression, all mice (including mCherry-expressing controls) were given CNO in their drinking water for 2 weeks. Mice were then behaviorally tested 20 min following an intraperitoneal (i.p.) CNO injection (Figure 7A). This procedure was designed to achieve brain-wide Tac2 overexpression and/or neuronal activation in Tac2$^+$ cells, during both a 2-week mock SIS period, as well as during behavioral testing.

Remarkably, combined overexpression of Tac2 and chemogenetic activation of Tac2$^+$ neurons recapitulated key behavioral effects of SIS in GH mice, including increased aggression and persistent freezing to threats (Figures 7B–7D; summarized in Figure 7F). In contrast, increasing Tac2 expression, or activating Tac2$^+$ neurons, on its own was insufficient to yield SIS-like effects in any of our assays (Figures 7B–7E, lavender and cyan bars), as was injection of mCherry-only virus. Histological analysis confirmed expression of mCherry-tagged AAV cargo genes in the dBNSTa, CeA, and DMH (Figures S7A–S7C) and in several

(G–J) Effect of osanetant administered during SIS on (G) aggression, (H) post-loom freezing, and (I) post-tone freezing. (J) Shock reactivity; a trend to protection (SIS-veh vs. osan during) was observed but did not reach our significance threshold ($p > 0.05$).

(K) Summary of results. "osan pre-test" indicates osanetant was given 20 min prior to each assay (B–E), but not during SIS; "osan during SIS" indicates osanetant was given during SIS only (G–J), and not 20 min before each assay. Faint red arrows indicate original effects produced by SIS. Black X's indicate SIS-induced effects that were blocked by the manipulation. n.c., no change.

See also Figure S3.

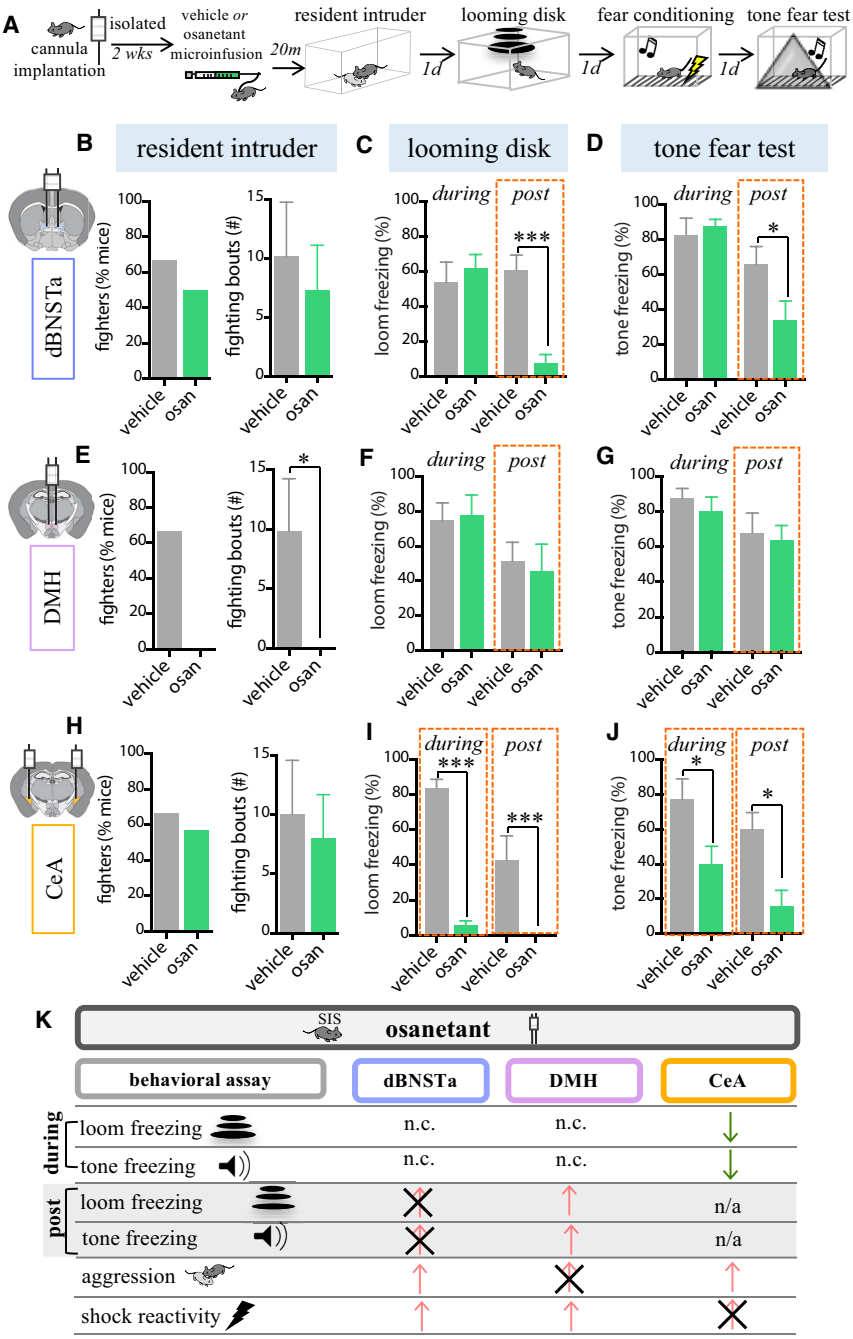

Figure 4. Targeted NK3R Antagonism in dBNSTa, DMH, or CeA Attenuates Different Effects of SIS in a Dissociable Manner

(A) Experimental protocol. Mice were implanted with bilateral cannulae in dBNSTa, DMH, or CeA; isolated; and given osanetant or vehicle microinfusions (300 nl) 20 min before testing (n = 6–7/condition).

(B–J) Effect of osanetant infusion into dBNSTa (B–D), DMH (E–G) or CeA (H–J) on indicated assays. Osanetant (green bars) selectively blocked persistent freezing in dBNSTa ("post"; C and D), aggression in DMH (E), and acute freezing in CeA ("during"; I and J).

(K) Summary of results. Notations are the same as those used in Figure 3K. n/a, not applicable (secondary to lack of freezing during stimulus). n.c., no change. Green downward arrows indicate manipulation-induced reduction in a behavior not altered by SIS.

See also Figure S4.

additional regions (Figures S7D and S7E). The absence of any effects in CNO-treated mCherry virus-injected mice rules out off-target effects of the drug (Gomez et al., 2017).

DISCUSSION

Identification of Tac2/NkB as a Key Mediator of Brain Responses to Chronic SIS

A large number of neuropeptides have been implicated in stress responses, most prominently CRH (reviewed in (Kormos and Gaszner, 2013; Kash et al., 2015; Chen, 2016)). Prior work on the tachykinins in stress has focused primarily on Tac1/Substance P/NkA (Bilkei-Gorzo et al., 2002; Beaujouan et al., 2004; Ebner et al., 2004, 2008). Previous pharmacological and genetic studies have yielded conflicting results regarding the direction of NkB influences on stress responses (Ebner et al., 2009). Motivated by our previous results in *Drosophila* (Asahina et al., 2014), we identified Tac2/NkB as an important and previously unrecognized mediator of chronic SIS influences on the brain. The finding that tachykinins play a role in the control of social isolation-induced aggression in both flies and mice is consistent with evidence supporting an evolutionary conservation of neuropeptide function in behavior across phylogeny (reviewed in Bargmann [2012]; Katz and Lillvis [2014]). It is conceivable that Tac2/NkB may play a role in the well-known effect of solitary confinement to increase violence in humans (Arrigo and Bullock, 2008).

CRH is considered the prototypic stress peptide (Chen, 2016). Approximately 50% of Tac2$^+$ cells in dBNSTa and CeA co-express CRH (Figure S7F), raising the possibility that co-release of CRH may play some role in effects of SIS exerted via these structures. However, Tac2 shRNAi and osanetant injections yielded similar effects as Tac2$^+$ neuronal silencing, while activation of Tac2$^+$ neurons had no effect unless a Tac2 cDNA was co-expressed. Therefore co-release of CRH is unlikely to explain the results of our chemogenetic manipulations of Tac2$^+$ neuronal activity. Nevertheless, we cannot exclude that CRH may act genetically upstream or downstream of Tac2 in these structures, to mediate the influences of SIS. Interestingly, there was virtually

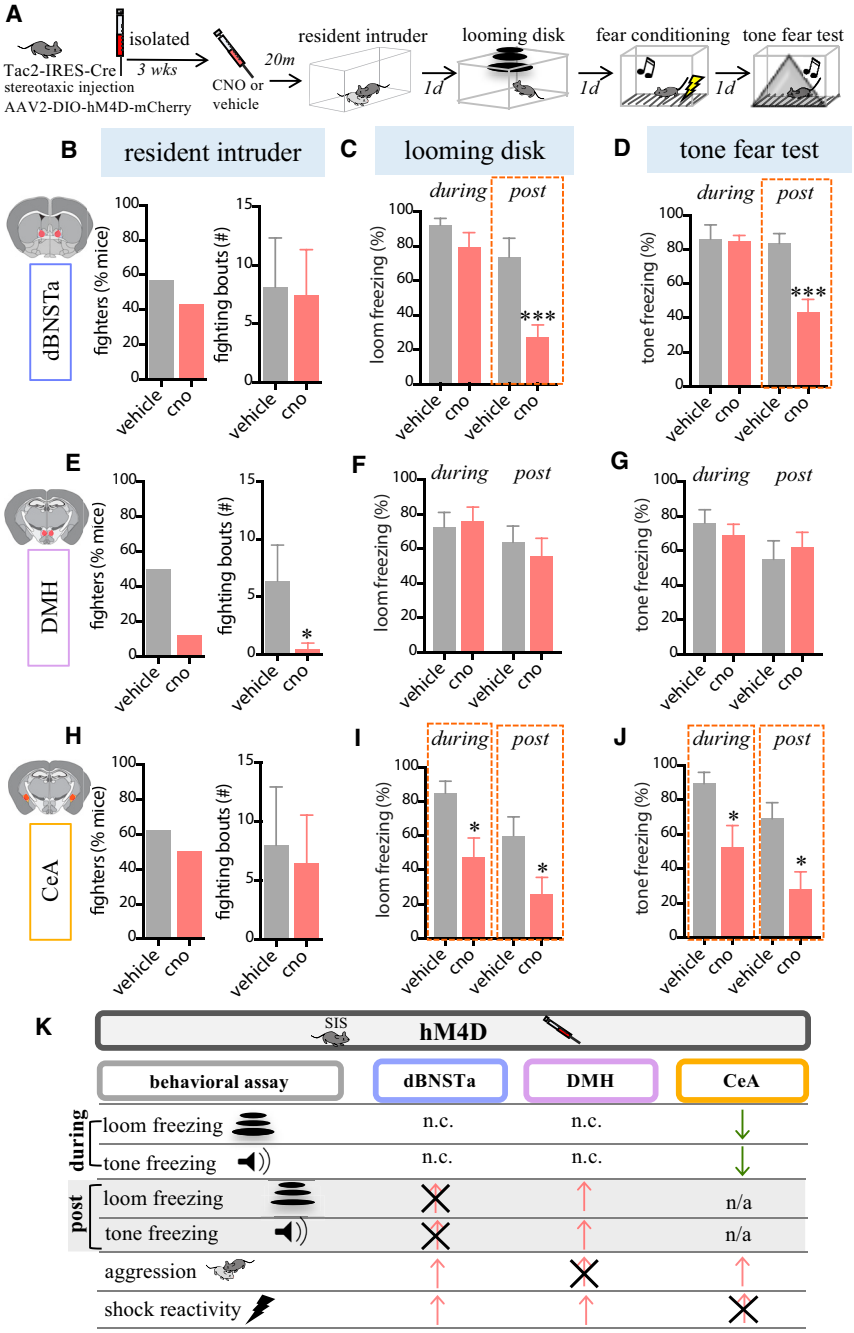

Figure 5. Targeted Chemogenetic Silencing of Tac2$^+$ Cells Attenuates the Effects of SIS

(A) Experimental protocol. Tac2-Cre mice were bilaterally injected in the indicated regions with a Cre-dependent AAV-expressing hM4DREADD-mCherry, isolated, and injected (i.p.) with CNO or vehicle prior to testing (n = 7–8 mice/condition).

(B–J) Effect of vehicle or CNO on mice expressing Tac2-hM4DREADD in dBNSTa (B–D), DMH (E–G), or CeA (H–J) on indicated assays. CNO blocked persistent freezing in dBNSTa ("post"; C and D), aggression in DMH (E), and acute freezing in CeA ("during"; I and J).

(K) Summary of results. Notations are the same as those used in Figure 4K. CNO had no effect in mCherry-expressing mice (Figure S5E).

See also Figure S5.

no expression of CRH among Tac2$^+$ neurons in DMH, where NkB controls aggression (Figure S7F).

Our SIS paradigm differs from acute and repeated intermittent stressors (e.g., footshock, restraint, forced swim) not only in its quality but also in its extended duration and continuous nature. The engagement of the Tac2/NkB system in chronic SIS, therefore, could reflect any of these differences. However, the fact that systemic delivery of osanetant blocked acute footshock-induced persistent freezing in the LD assay suggests a more general role for the peptide in responses to stressors. A role for Tac2/NkB in consolidation of a conditioned fear memory in CeA has been reported (Andero et al., 2014), but this effect was interpreted to reflect a role in memory consolidation. Understanding the role of Tac2 in other forms of chronic and acute stress will be an interesting topic for future studies.

Tac2/NkB Acts in a Distributed Manner to Control Multiple Components of the SIS Response

With few exceptions (Regev et al., 2011, 2012), most previous studies of neuropeptides in stress have focused on a single brain region, stressor and/or behavior (e.g., the BNST and anxiety assays; reviewed in Kash et al. [2015]), and have used a single type of functional perturbation (but see McCall et al. [2015]). This, together with the variations in stress and behavioral paradigms used in different laboratories, makes it difficult to synthesize studies of the same peptide in different regions to understand how a peptide acts more globally in the brain (Kormos and Gaszner, 2013; Chen, 2016). The multiplexed approach used here permitted comparison of the same perturbation in different brain regions, and of different perturbations in the same brain region, using a battery of behavioral assays. This approach revealed a distributed mode of action in which upregulation of Tac2 by stress regulated different behavioral effects of SIS in different areas. Such a distributed mechanism is reminiscent of that played by pigment-dispersing factor (PDF) in controlling circadian circuits in *Drosophila* (Taghert and Nitabach, 2012; Dubowy and Sehgal, 2017), or roaming versus

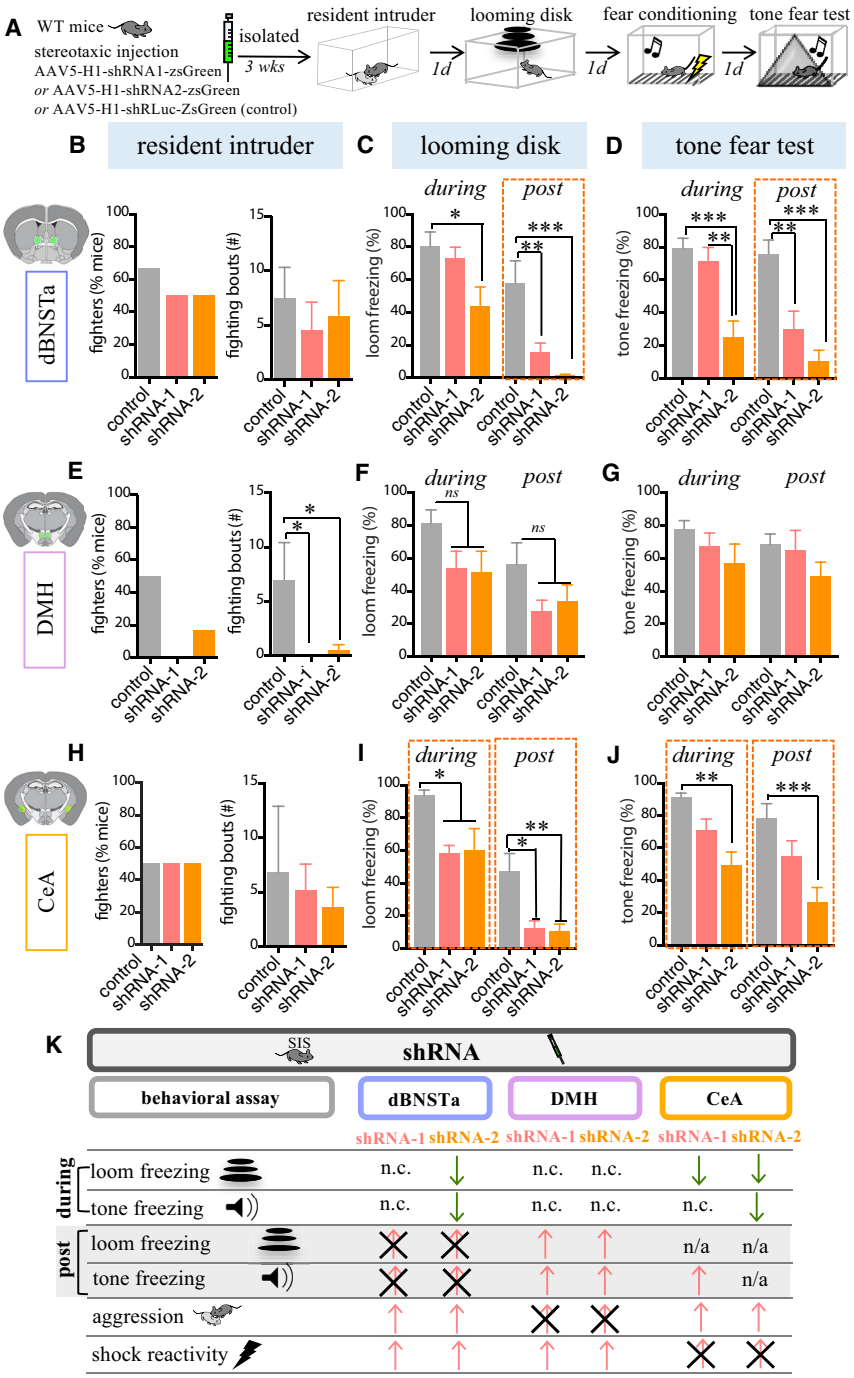

Figure 6. Targeted Knockdown of Tac2 Attenuates the Effects of SIS

(A) Experimental protocol. 3 weeks prior to testing, wild-type (WT) mice were injected with an AAV-expressing shRNA-zsGreen for specific knockdown of Tac2 (shRNA-1 or shRNA-2) or with an shRNA virus targeting the luciferase gene (control) (n = 6–7/mice condition) and maintained in isolation until testing.

(B–J) Effect of shRNA's in dBNSTa (B–D), DMH (E–G), or CeA (H–J) on indicated assays. shRNA-1 (red bars) blocked persistent freezing in dBNSTa ("post"; C and D); aggression in DMH (E) and freezing in CeA (I–J). shRNA-2 (orange bars) yielded similar effects but additionally reduced acute freezing in dBNSTa ("during"; C and D).

(K) Summary of the results. The effects of shRNA-1 (left column) and shRNA-2 (right column) are presented for each region.

See also Figure S6.

dwelling states in *C. elegans* (Flavell et al., 2013), and may also explain some of the diverse functions of CRH (Regev et al., 2011; Flandreau et al., 2012; McCall et al., 2015).

The fact that local inhibition of Tac2/NkB synthesis, Tac2$^+$ neuronal activity and NkB receptors yielded qualitatively similar results in each brain region is suggestive of local actions of Tac2. In other systems, NkB acts in an autocrine or paracrine manner on Nk3R-expressing neurons to increase their activity (Navarro, 2013); whether this occurs in the regions studied here is not yet clear. Importantly, our results do not rule out requirements for NkB signaling at distal targets of Tac2$^+$ neurons as well. The biochemistry of Nk3R action suggests that Tac2/NkB should increase intracellular free calcium via an IP3/DAG pathway (Ebner et al., 2009). In this way, NkB could potentiate the activation of target neurons by glutamate or other excitatory transmitters, and/or promote release of additional peptides.

Activation and Peptide Overexpression in Tac2$^+$ Neurons Mimics the Effects of SIS

Injection of stress peptides or receptor agonists can elicit behavioral responses (reviewed in Koob [1999]; Bruchas et al. [2010]; Kormos and Gaszner [2013]). However, in most studies, injection or transgenic overexpression of a stress peptide does not fully mimic the behavioral effects of stressors. For example, even CRH when exogenously administered to unstressed animals in low arousal conditions does not produce stress-like responses (Koob, 1999).

Using a novel experimental design, we found that overexpression of Tac2 combined with neuronal activation in Tac2$^+$ cells, but neither manipulation on its own, sufficed to mimic several of the behavioral effects of SIS, in GH mice. This suggests that neuronal activity may be limiting for observing behavioral effects of neuropeptide overexpression in other systems. This may explain why overexpression of CRH using genetic methods produced different responses, depending on the mode and site of expression (Regev et al., 2011, 2012; Flandreau et al., 2012; Sink et al., 2013; Kash et al., 2015).

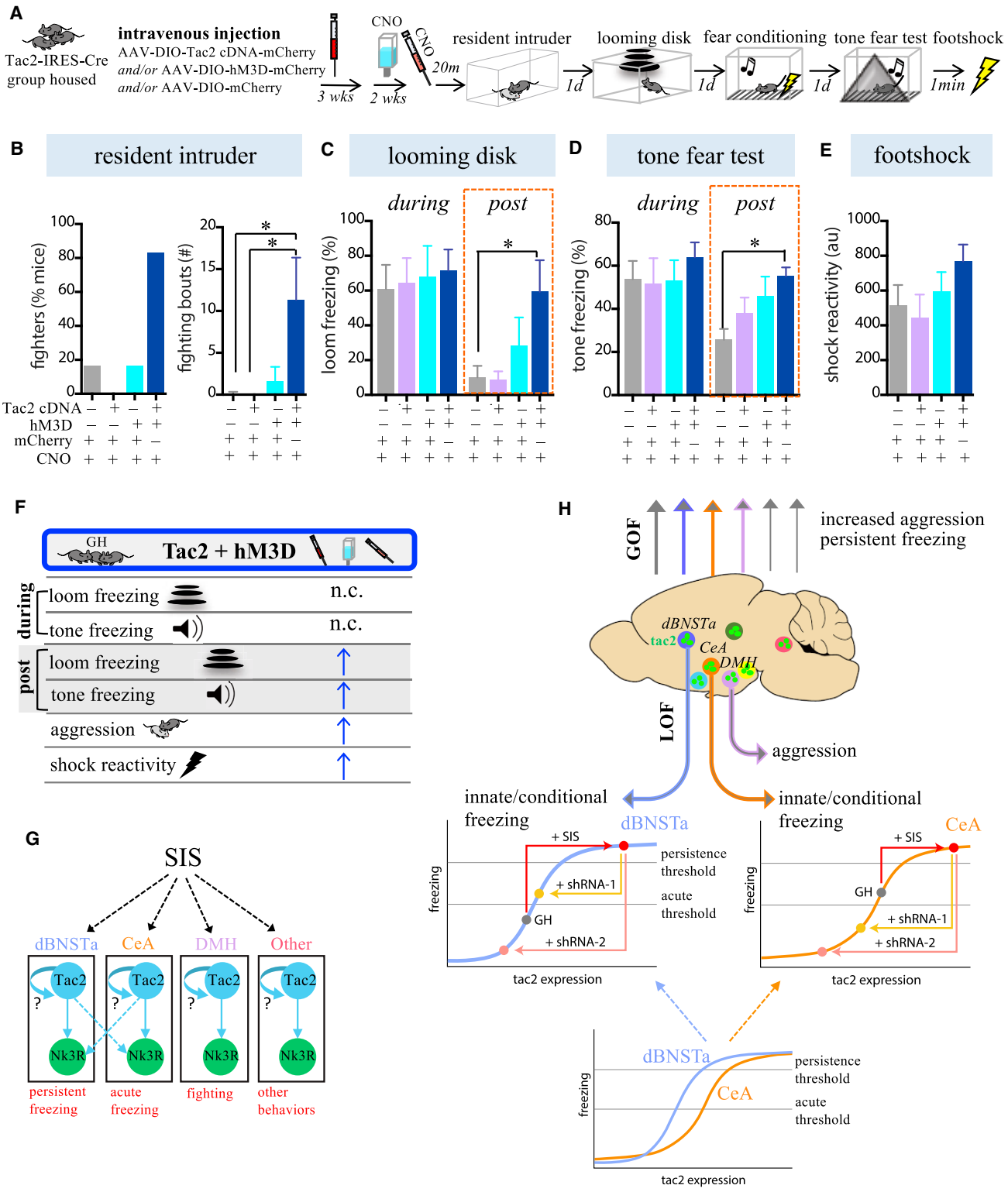

Figure 7. Activation of Tac2^{+} Neurons plus Tac2 Overexpression Mimics the Effects of SIS in GH Mice

(A) Experimental protocol. GH Tac2-IRES-Cre mice were intravenously injected with Cre-dependent, human Synapsin I promoter-driven, and AAV-PHP.B-serotyped viruses expressing the chemogenetic activator hM3DREADD, a Tac2 cDNA, both, or just mCherry (controls). Mice remained group housed (5 weeks) with CNO-spiked drinking water provided during the final 2 weeks (for hM3DREADD activation). Mice received an injection of CNO (i.p.) 20 min prior to each assay (n = 6 mice/condition).

(legend continued on next page)

Our experiments were enabled by a strategy that allows independent manipulation of Tac2 expression and $Tac2^{+}$ neuronal activity, in a brain-wide, non-invasive manner in adult mice (Deverman et al., 2016; Chan et al., 2017), without the need to employ complex transgenic strategies (Lu et al., 2008). More spatially and temporally resolved applications of this approach should reveal precisely where and when enhancing NkB signaling exerts its effects. We anticipate that this approach will prove useful for studying other neuropeptides as well.

Increased Tac2/NkB Signaling Converts Stimulus-Locked to Persistent Threat Responses

It was striking to observe that acute freezing responses to threats in GH animals could be converted to persistent ones, simply by artificially increasing Tac2 expression and release. Preliminary data indicate that Tac2 is required for acute freezing in GH animals as well. Together, these data suggest that the upregulation of Tac2 expression caused by SIS may serve to convert defensive reactions to threats from transient to more enduring responses (Figure 7H, lower). In this way, the scalable property of neuropeptides—their concentration can vary continuously—may be used to promote persistence, a key component of emotion and related internal states (Anderson and Adolphs, 2014).

With one exception (see below), manipulations of NkB signaling in dBNSTa reduced persistent, but not acute (during stimulus) freezing, while manipulations of CeA reduced freezing during as well as following threat stimulus presentation. This dissociation appears consistent with the prevailing view that CeA controls phasic, stimulus-locked defensive responses to threats ("fear"), while dBNSTa controls more persistent responses ("anxiety") (Walker et al., 2009; Kash et al., 2015). However, in dBNSTa the more potent Tac2 shRNA-2 inhibited acute as well as persistent freezing, while the less potent shRNA-1 only reduced post-stimulus freezing. These data suggest that the effects of Tac2/NkB signaling on acute versus enduring responses to threats are not determined simply by the region(s) in which the neuropeptide acts but also by the level of peptide expression and by potentially different thresholds for neuropeptide effects in each area (Figure 7H). However, we cannot exclude the possibility that reciprocal connections between CeA and dBNST (Dong et al., 2001; Dong and Swanson, 2006a, 2006b) may also contribute to the partially overlapping shRNAi phenotypes we observed (Figure 7G).

Nk3R Antagonists as a Potential Treatment for Isolation-Related Stress

Social isolation is well known to promote poor health, clinical psychiatric symptoms, and increased mortality in humans (Cacioppo and Hawkley, 2009; Umberson and Montez, 2010; Cacioppo et al., 2015; Holt-Lunstad et al., 2015). Osanetant and several other Nk3R antagonists have been tested in clinical trials as therapies for schizophrenia, bipolar, and panic disorder (Spooren et al., 2005). These drugs were well tolerated but abandoned for lack of efficacy (Griebel and Holsboer, 2012). The profound effect of osanetant to prevent and attenuate an SIS-induced deleterious brain state suggests that Nk3R antagonists may merit re-examination as potential treatments for mood disorders caused by extended periods of social isolation (or other stressors) in humans, and in domesticated animals as well.

STAR★METHODS

Detailed methods are provided in the online version of this paper and include the following:

- KEY RESOURCES TABLE
- CONTACT FOR REAGENT AND RESOURCE SHARING
- EXPERIMENTAL MODEL AND SUBJECT DETAILS
  - Animals
  - Social isolation stress
- METHOD DETAILS
  - Viral constructs
  - Construction of small hairpin RNA expressing AAV vector
  - Construction of Tac2-overexpression AAV vectors
  - Viral packaging
  - AAV-PHP.B production and intravenous administration
  - Surgery and cannula implants
  - Immunohistochemistry
  - Fluorescent *in situ* hybridization
  - Cell counting
  - Quantitative real-time reverse transcription PCR
  - Resident intruder assay
  - Looming disk assay
  - Tone fear conditioning and shock reactivity
  - Ultrasonic sound stimulus assay
  - Open field test
  - Elevated plus maze
  - Acoustic startle response
  - Flinch-vocalize-jump assay
  - Social interaction assay
  - Rat exposure assay
  - Pharmacology
- QUANTIFICATION AND STATISTICAL ANALYSIS

(B–E) Effect of each manipulation on the indicated assays. All animals were treated with CNO and received the same total amount of the virus. Only mice receiving both the hM3DREADD and Tac2 cDNA viruses showed an "SIS-like" phenotype (dark blue bars), including increased aggression (B), post-loom freezing (C), and post-tone freezing (D). (E) Reactivity to the footshock.

(F) Summary of results. Blue arrows indicate effects of perturbations to generate SIS-like effects.

(G) Schematic illustrating how Tac2 and its receptor (Nk3R) may control SIS-induced behavior.

(H) Upper: illustration summarizing LOF and GOF effects on behavior. Lower: model graphs showing how different thresholds for acute versus persistent freezing and different dose dependencies of freezing on Tac2 levels in dBNSTa versus CeA (bottom graph) could explain the differential effects of shRNA −1 (weaker) and −2 (stronger; upper graphs) in the two regions (see Figure 6). The model also illustrates how an increase in Tac2 levels caused by SIS (red line) could convert acute (CeA-dependent) to persistent (dBNSTa-dependent) freezing. Gray dot, baseline levels of Tac2 in GH mice are higher in CeA than in dBNSTa, based on FISH data (Figures 2L and 2N).

See also Figure S7.

SUPPLEMENTAL INFORMATION

Supplemental Information includes seven figures and two tables and can be found with this article online at https://doi.org/10.1016/j.cell.2018.03.037.

ACKNOWLEDGMENTS

We thank X. Da and X. Wang for help with behavior scoring and histology; M. McCardle and Y. Huang for genotyping; J. Costanza for mouse colony management; C. Chiu and G. Mancuso for lab management and administrative assistance; A. Choe for help with behavioral testing, the diagrams in Figure 2A, and fruitful discussions; A. Kennedy for generating MATLAB code for behavioral data processing and the models in Figure 7H; Z. Turan and M. Meister for help implementing the LD assay; W. Wu for initial help on the acoustic startle assay; P. Kunwar for initial help on the ultrasonic sound stimulus assay; T. Anthony for initial help with RNA isolation and purification; and all the members of the Anderson lab for their support. We thank Ben Deneen for providing the NFIA antibody, Mitchell Guttman and his lab for providing resources and sharing use of the qRT-PCR reagents and equipment, the Beckman Institute CLOVER Center for generating the PHP.B constructs, and the Perona lab for continued help with customized behavioral tracking and analyses software. This work was supported by grants from the National Institutes Health (MH085082, MH112593, and MH070053), Gordon Moore Foundation (2646), Ellison Medical Research Foundation (NR-AA-0108-12), and Simons Foundation (to D.J.A.) and by a NARSAD Young Investigator Award (23687), the L'OREAL for Women in Science award, and an NIMH K99 Pathway to Independence Award (MH108734 to M.Z.). D.J.A. is an Investigator of the Howard Hughes Medical Institute.

AUTHOR CONTRIBUTIONS

M.Z. and D.J.A. contributed to the study design. M.Z., M.H., A.C., M.R.B., and B.E.D. contributed to the data collection, scoring, and analysis. M.Z. and M.H. conducted the surgeries, behavior experiments, and histological analyses. K.B. performed PHP.B viral packaging, and B.E.D. helped design the PHP.B experiments and performed the retro-orbital viral injections. T.K. contributed the shRNA and Tac2 cDNA constructs. B.Y. contributed to packaging the viral constructs. M.R.B. contributed to the qRT-PCR analyses. V.G. provided funding to support K.B. and B.E.D. and provided comments on the manuscript. M.Z. and D.J.A. wrote the paper. All authors discussed and commented on the manuscript.

DECLARATION OF INTERESTS

B.E.D. and V.G. are listed as inventors on a patent related to AAV-PHP.B (#US9585971B2). All other authors declare no competing interests.

Received: September 27, 2017
Revised: January 29, 2018
Accepted: March 15, 2018
Published: May 17, 2018

REFERENCES

An, D., Chen, W., Yu, D.Q., Wang, S.W., Yu, W.Z., Xu, H., Wang, D.M., Zhao, D., Sun, Y.P., Wu, J.C., Tang, Y.Y., and Yin, S.M. (2017). Effects of social isolation, re-socialization and age on cognitive and aggressive behaviors of Kunming mice and BALB/c mice. Anim. Sci. J. *88*, 798–806.

Andero, R., Dias, B.G., and Ressler, K.J. (2014). A role for Tac2, NkB, and Nk3 receptor in normal and dysregulated fear memory consolidation. Neuron *83*, 444–454.

Andero, R., Daniel, S., Guo, J.D., Bruner, R.C., Seth, S., Marvar, P.J., Rainnie, D., and Ressler, K.J. (2016). Amygdala-dependent molecular mechanisms of the Tac2 pathway in fear learning. Neuropsychopharmacology *41*, 2714–2722.

Anderson, D.J. (2016). Circuit modules linking internal states and social behaviour in flies and mice. Nat. Rev. Neurosci. *17*, 692–704.

Anderson, D.J., and Adolphs, R. (2014). A framework for studying emotions across species. Cell *157*, 187–200.

Anthony, T.E., Dee, N., Bernard, A., Lerchner, W., Heintz, N., and Anderson, D.J. (2014). Control of stress-induced persistent anxiety by an extra-amygdala septohypothalamic circuit. Cell *156*, 522–536.

Arrigo, B.A., and Bullock, J.L. (2008). The psychological effects of solitary confinement on prisoners in supermax units: reviewing what we know and recommending what should change. Int. J. Offender Ther. Comp. Criminol. *52*, 622–640.

Asahina, K., Watanabe, K., Duistermars, B.J., Hoopfer, E., González, C.R., Eyjólfsdóttir, E.A., Perona, P., and Anderson, D.J. (2014). Tachykinin-expressing neurons control male-specific aggressive arousal in Drosophila. Cell *156*, 221–235.

Bargmann, C.I. (2012). Beyond the connectome: how neuromodulators shape neural circuits. BioEssays *34*, 458–465.

Beaujouan, J.C., Torrens, Y., Saffroy, M., Kemel, M.L., and Glowinski, J. (2004). A 25 year adventure in the field of tachykinins. Peptides *25*, 339–357.

Berridge, K.C. (2004). Motivation concepts in behavioral neuroscience. Physiol. Behav. *81*, 179–209.

Bilkei-Gorzo, A., Racz, I., Michel, K., and Zimmer, A. (2002). Diminished anxiety- and depression-related behaviors in mice with selective deletion of the Tac1 gene. J. Neurosci. *22*, 10046–10052.

Blanchard, D.C., Griebel, G., and Blanchard, R.J. (2003). The mouse defense test battery: pharmacological and behavioral assays for anxiety and panic. Eur. J. Pharmacol. *463*, 97–116.

Blanchard, D.C., Blanchard, R.J., and Griebel, G. (2005). Defensive responses to predator threat in the rat and mouse. Curr. Protoc. Neurosci *Chapter 8*, Unit 8.19.

Bourin, M., Petit-Demoulière, B., Dhonnchadha, B.N., and Hascöet, M. (2007). Animal models of anxiety in mice. Fundam. Clin. Pharmacol. *21*, 567–574.

Bruchas, M.R., Land, B.B., and Chavkin, C. (2010). The dynorphin/kappa opioid system as a modulator of stress-induced and pro-addictive behaviors. Brain Res. *1314*, 44–55.

Cacioppo, J.T., and Hawkley, L.C. (2009). Perceived social isolation and cognition. Trends Cogn. Sci. *13*, 447–454.

Cacioppo, S., Capitanio, J.P., and Cacioppo, J.T. (2014). Toward a neurology of loneliness. Psychol. Bull. *140*, 1464–1504.

Cacioppo, J.T., Cacioppo, S., Capitanio, J.P., and Cole, S.W. (2015). The neuroendocrinology of social isolation. Annu. Rev. Psychol. *66*, 733–767.

Cai, H., Haubensak, W., Anthony, T.E., and Anderson, D.J. (2014). Central amygdala PKC-δ(+) neurons mediate the influence of multiple anorexigenic signals. Nat. Neurosci. *17*, 1240–1248.

Chan, K.Y., Jang, M.J., Yoo, B.B., Greenbaum, A., Ravi, N., Wu, W.L., Sánchez-Guardado, L., Lois, C., Mazmanian, S.K., Deverman, B.E., and Gradinaru, V. (2017). Engineered AAVs for efficient noninvasive gene delivery to the central and peripheral nervous systems. Nat. Neurosci. *20*, 1172–1179.

Chen, A. (2016). Genetic dissection of the neuroendocrine and behavioral responses to stressful challenges. In Stem Cells in Neuroendocrinology, D. Pfaff and Y. Christen, eds. (Springer).

Cho, J.R., Treweek, J.B., Robinson, J.E., Xiao, C., Bremner, L.R., Greenbaum, A., and Gradinaru, V. (2017). Dorsal raphe dopamine neurons modulate arousal and promote wakefulness by salient stimuli. Neuron *94*, 1205–1219.e8.

Conklin, B.R., Hsiao, E.C., Claeysen, S., Dumuis, A., Srinivasan, S., Forsayeth, J.R., Guettier, J.M., Chang, W.C., Pei, Y., McCarthy, K.D., et al. (2008). Engineering GPCR signaling pathways with RASSLs. Nat. Methods *5*, 673–678.

Culman, J., and Unger, T. (1995). Central tachykinins: mediators of defence reaction and stress reactions. Can. J. Physiol. Pharmacol. *73*, 885–891.

Cushman, J.D., Moore, M.D., Olsen, R.W., and Fanselow, M.S. (2014). The role of the δ GABA(A) receptor in ovarian cycle-linked changes in hippocampus-dependent learning and memory. Neurochem. Res. *39*, 1140–1146.

Deneen, B., Ho, R., Lukaszewicz, A., Hochstim, C.J., Gronostajski, R.M., and Anderson, D.J. (2006). The transcription factor NFIA controls the onset of gliogenesis in the developing spinal cord. Neuron *52*, 953–968.

Deverman, B.E., Pravdo, P.L., Simpson, B.P., Kumar, S.R., Chan, K.Y., Banerjee, A., Wu, W.L., Yang, B., Huber, N., Pasca, S.P., and Gradinaru, V. (2016). Cre-dependent selection yields AAV variants for widespread gene transfer to the adult brain. Nat. Biotechnol. *34*, 204–209.

Dong, H.-W., and Swanson, L.W. (2006a). Projections from bed nuclei of the stria terminalis, anteromedial area: cerebral hemisphere integration of neuroendocrine, autonomic, and behavioral aspects of energy balance. J. Comp. Neurol. *494*, 142–178.

Dong, H.-W., and Swanson, L.W. (2006b). Projections from bed nuclei of the stria terminalis, dorsomedial nucleus: implications for cerebral hemisphere integration of neuroendocrine, autonomic, and drinking responses. J. Comp. Neurol. *494*, 75–107.

Dong, H.W., Petrovich, G.D., and Swanson, L.W. (2001). Topography of projections from amygdala to bed nuclei of the stria terminalis. Brain Res. Brain Res. Rev. *38*, 192–246.

Dubowy, C., and Sehgal, A. (2017). Circadian rhythms and sleep in Drosophila melanogaster*205* (Genetics), pp. 1373–1397.

Ebner, K., Rupniak, N.M., Saria, A., and Singewald, N. (2004). Substance P in the medial amygdala: emotional stress-sensitive release and modulation of anxiety-related behavior in rats. Proc. Natl. Acad. Sci. USA *101*, 4280–4285.

Ebner, K., Muigg, P., Singewald, G., and Singewald, N. (2008). Substance P in stress and anxiety: NK-1 receptor antagonism interacts with key brain areas of the stress circuitry. Ann. N Y Acad. Sci. *1144*, 61–73.

Ebner, K., Sartori, S.B., and Singewald, N. (2009). Tachykinin receptors as therapeutic targets in stress-related disorders. Curr. Pharm. Des. *15*, 1647–1674.

Emonds-Alt, X., Bichon, D., Ducoux, J.P., Heaulme, M., Miloux, B., Poncelet, M., Proietto, V., Van Broeck, D., Vilain, P., Neliat, G., et al. (1995). SR 142801, the first potent non-peptide antagonist of the tachykinin NK3 receptor. Life Sci. *56*, PL27–PL32.

Fanselow, M.S. (1980). Conditioned and unconditional components of post-shock freezing. Pavlov. J. Biol. Sci. *15*, 177–182.

Flandreau, E.I., Ressler, K.J., Owens, M.J., and Nemeroff, C.B. (2012). Chronic overexpression of corticotropin-releasing factor from the central amygdala produces HPA axis hyperactivity and behavioral anxiety associated with gene-expression changes in the hippocampus and paraventricular nucleus of the hypothalamus. Psychoneuroendocrinology *37*, 27–38.

Flavell, S.W., Pokala, N., Macosko, E.Z., Albrecht, D.R., Larsch, J., and Bargmann, C.I. (2013). Serotonin and the neuropeptide PDF initiate and extend opposing behavioral states in C. elegans. Cell *154*, 1023–1035.

Gomez, J.L., Bonaventura, J., Lesniak, W., Mathews, W.B., Sysa-Shah, P., Rodriguez, L.A., Ellis, R.J., Richie, C.T., Harvey, B.K., Dannals, R.F., et al. (2017). Chemogenetics revealed: DREADD occupancy and activation via converted clozapine. Science *357*, 503–507.

Griebel, G., and Holsboer, F. (2012). Neuropeptide receptor ligands as drugs for psychiatric diseases: the end of the beginning? Nat. Rev. Drug Discov. *11*, 462–478.

Haubensak, W., Kunwar, P.S., Cai, H., Ciocchi, S., Wall, N.R., Ponnusamy, R., Biag, J., Dong, H.W., Deisseroth, K., Callaway, E.M., et al. (2010). Genetic dissection of an amygdala microcircuit that gates conditioned fear. Nature *468*, 270–276.

Hawkley, L.C., Cole, S.W., Capitanio, J.P., Norman, G.J., and Cacioppo, J.T. (2012). Effects of social isolation on glucocorticoid regulation in social mammals. Horm. Behav. *62*, 314–323.

Hilakivi, L.A., Ota, M., and Lister, R.G. (1989). Effect of isolation on brain monoamines and the behavior of mice in tests of exploration, locomotion, anxiety and behavioral 'despair'. Pharmacol. Biochem. Behav. *33*, 371–374.

Holt-Lunstad, J., Smith, T.B., and Layton, J.B. (2010). Social relationships and mortality risk: a meta-analytic review. PLoS Med. *7*, e1000316.

Holt-Lunstad, J., Smith, T.B., Baker, M., Harris, T., and Stephenson, D. (2015). Loneliness and social isolation as risk factors for mortality: a meta-analytic review. Perspect. Psychol. Sci. *10*, 227–237.

Hong, W., Kim, D.W., and Anderson, D.J. (2014). Antagonistic control of social versus repetitive self-grooming behaviors by separable amygdala neuronal subsets. Cell *158*, 1348–1361.

Hong, W., Kennedy, A., Burgos-Artizzu, X.P., Zelikowsky, M., Navonne, S.G., Perona, P., and Anderson, D.J. (2015). Automated measurement of mouse social behaviors using depth sensing, video tracking, and machine learning. Proc. Natl. Acad. Sci. USA *112*, E5351–E5360.

House, J.S., Landis, K.R., and Umberson, D. (1988). Social relationships and health. Science *241*, 540–545.

Hsiao, E.Y., McBride, S.W., Hsien, S., Sharon, G., Hyde, E.R., McCue, T., Codelli, J.A., Chow, J., Reisman, S.E., Petrosino, J.F., et al. (2013). Microbiota modulate behavioral and physiological abnormalities associated with neurodevelopmental disorders. Cell *155*, 1451–1463.

Kash, T.L., Pleil, K.E., Marcinkiewcz, C.A., Lowery-Gionta, E.G., Crowley, N., Mazzone, C., Sugam, J., Hardaway, J.A., and McElligott, Z.A. (2015). Neuropeptide regulation of signaling and behavior in the BNST. Mol. Cells *38*, 1–13.

Katz, P.S., and Lillvis, J.L. (2014). Reconciling the deep homology of neuromodulation with the evolution of behavior. Curr. Opin. Neurobiol. *29*, 39–47.

Katz, R.J., Roth, K.A., and Carroll, B.J. (1981). Acute and chronic stress effects on open field activity in the rat: implications for a model of depression. Neurosci. Biobehav. Rev. *5*, 247–251.

Kessler, R.C., Aguilar-Gaxiola, S., Alonso, J., Chatterji, S., Lee, S., Ormel, J., Ustün, T.B., and Wang, P.S. (2009). The global burden of mental disorders: an update from the WHO World Mental Health (WMH) surveys. Epidemiol. Psichiatr. Soc. *18*, 23–33.

Kim, J.J., DeCola, J.P., Landeira-Fernandez, J., and Fanselow, M.S. (1991). N-methyl-D-aspartate receptor antagonist APV blocks acquisition but not expression of fear conditioning. Behav. Neurosci. *105*, 126–133.

Kim, J., Zhang, X., Muralidhar, S., LeBlanc, S.A., and Tonegawa, S. (2017). Basolateral to central amygdala neural circuits for appetitive behaviors. Neuron *93*, 1464–1479.e5.

Koch, M. (1999). The neurobiology of startle. Prog. Neurobiol. *59*, 107–128.

Koob, G.F. (1999). Corticotropin-releasing factor, norepinephrine, and stress. Biol. Psychiatry *46*, 1167–1180.

Kormos, V., and Gaszner, B. (2013). Role of neuropeptides in anxiety, stress, and depression: from animals to humans. Neuropeptides *47*, 401–419.

Kunwar, P.S., Zelikowsky, M., Remedios, R., Cai, H., Yilmaz, M., Meister, M., and Anderson, D.J. (2015). Ventromedial hypothalamic neurons control a defensive emotion state. eLife *4*, 4.

LeDoux, J. (2012). Rethinking the emotional brain. Neuron *73*, 653–676.

Lee, H., Kim, D.W., Remedios, R., Anthony, T.E., Chang, A., Madisen, L., Zeng, H., and Anderson, D.J. (2014). Scalable control of mounting and attack by Esr1+ neurons in the ventromedial hypothalamus. Nature *509*, 627–632.

Lein, E.S., Hawrylycz, M.J., Ao, N., Ayres, M., Bensinger, A., Bernard, A., Boe, A.F., Boguski, M.S., Brockway, K.S., Byrnes, E.J., et al. (2007). Genome-wide atlas of gene expression in the adult mouse brain. Nature *445*, 168–176.

Lu, A., Steiner, M.A., Whittle, N., Vogl, A.M., Walser, S.M., Ableitner, M., Refojo, D., Ekker, M., Rubenstein, J.L., Stalla, G.K., et al. (2008). Conditional mouse mutants highlight mechanisms of corticotropin-releasing hormone effects on stress-coping behavior. Mol. Psychiatry *13*, 1028–1042.

Madisen, L., Zwingman, T.A., Sunkin, S.M., Oh, S.W., Zariwala, H.A., Gu, H., Ng, L.L., Palmiter, R.D., Hawrylycz, M.J., Jones, A.R., et al. (2010). A robust and high-throughput Cre reporting and characterization system for the whole mouse brain. Nat. Neurosci. *13*, 133–140.

Maggio, J.E. (1988). Tachykinins. Annu. Rev. Neurosci. *11*, 13–28.

Matsumoto, K., Pinna, G., Puia, G., Guidotti, A., and Costa, E. (2005). Social isolation stress-induced aggression in mice: a model to study the pharmacology of neurosteroidogenesis. Stress *8*, 85–93.

Matthews, G.A., Nieh, E.H., Vander Weele, C.M., Halbert, S.A., Pradhan, R.V., Yosafat, A.S., Glober, G.F., Izadmehr, E.M., Thomas, R.E., Lacy, G.D., et al. (2016). Dorsal raphe dopamine neurons represent the experience of social isolation. Cell *164*, 617–631.

McCall, J.G., Al-Hasani, R., Siuda, E.R., Hong, D.Y., Norris, A.J., Ford, C.P., and Bruchas, M.R. (2015). CRH engagement of the locus coeruleus noradrenergic system mediates stress-induced anxiety. Neuron*87*, pp. 605–620.

McEwen, B.S., Bowles, N.P., Gray, J.D., Hill, M.N., Hunter, R.G., Karatsoreos, I.N., and Nasca, C. (2015). Mechanisms of stress in the brain. Nat. Neurosci. *18*, 1353–1363.

Mongeau, R., Miller, G.A., Chiang, E., and Anderson, D.J. (2003). Neural correlates of competing fear behaviors evoked by an innately aversive stimulus. J. Neurosci. *23*, 3855–3868.

Naito, Y., Yoshimura, J., Morishita, S., and Ui-Tei, K. (2009). siDirect 2.0: updated software for designing functional siRNA with reduced seed-dependent off-target effect. BMC Bioinformatics *10*, 392.

Navarro, V.M. (2013). Interactions between kisspeptins and neurokinin B. Adv. Exp. Med. Biol. *784*, 325–347.

Regev, L., Neufeld-Cohen, A., Tsoory, M., Kuperman, Y., Getselter, D., Gil, S., and Chen, A. (2011). Prolonged and site-specific over-expression of corticotropin-releasing factor reveals differential roles for extended amygdala nuclei in emotional regulation. Mol. Psychiatry *16*, 714–728.

Regev, L., Tsoory, M., Gil, S., and Chen, A. (2012). Site-specific genetic manipulation of amygdala corticotropin-releasing factor reveals its imperative role in mediating behavioral response to challenge. Biol. Psychiatry *71*, 317–326.

Remedios, R., Kennedy, A., Zelikowsky, M., Grewe, B.F., Schnitzer, M.J., and Anderson, D.J. (2017). Social behaviour shapes hypothalamic neural ensemble representations of conspecific sex. Nature *550*, 388–392.

Sapolsky, R.M. (1996). Why stress is bad for your brain. Science *273*, 749–750.

Selye, H. (1936). A syndrome produced by diverse nocuous agents. Nature *138*, 32.

Shi, L., Fatemi, S.H., Sidwell, R.W., and Patterson, P.H. (2003). Maternal influenza infection causes marked behavioral and pharmacological changes in the offspring. J. Neurosci. *23*, 297–302.

Sink, K.S., Walker, D.L., Freeman, S.M., Flandreau, E.I., Ressler, K.J., and Davis, M. (2013). Effects of continuously enhanced corticotropin releasing factor expression within the bed nucleus of the stria terminalis on conditioned and unconditioned anxiety. Mol. Psychiatry *18*, 308–319.

Spooren, W., Riemer, C., and Meltzer, H. (2005). Opinion: NK3 receptor antagonists: the next generation of antipsychotics? Nat. Rev. Drug Discov. *4*, 967–975.

Taghert, P.H., and Nitabach, M.N. (2012). Peptide neuromodulation in invertebrate model systems. Neuron *76*, 82–97.

Tasic, B., Menon, V., Nguyen, T.N., Kim, T.K., Jarsky, T., Yao, Z., Levi, B., Gray, L.T., Sorensen, S.A., Dolbeare, T., et al. (2016). Adult mouse cortical cell taxonomy revealed by single cell transcriptomics. Nat. Neurosci. *19*, 335–346.

Thompson, C.L., Pathak, S.D., Jeromin, A., Ng, L.L., MacPherson, C.R., Mortrud, M.T., Cusick, A., Riley, Z.L., Sunkin, S.M., Bernard, A., et al. (2008). Genomic anatomy of the hippocampus. Neuron *60*, 1010–1021.

Thurmond, J.B. (1975). Technique for producing and measuring territorial aggression using laboratory mice. Physiol. Behav. *14*, 879–881.

Toth, M., Mikics, E., Tulogdi, A., Aliczki, M., and Haller, J. (2011). Post-weaning social isolation induces abnormal forms of aggression in conjunction with increased glucocorticoid and autonomic stress responses. Horm. Behav. *60*, 28–36.

Umberson, D., and Montez, J.K. (2010). Social relationships and health: a flashpoint for health policy. J. Health Soc. Behav. *51* (*Suppl*), S54–S66.

Valzelli, L. (1969). Aggressive behavior induced by isolation. In Aggressive Behavior, S. Garattini and E.B. Sigg, eds. (Excerpta Media).

Valzelli, L. (1973). The "isolation syndrome" in mice. Psychopharmacology (Berl.) *31*, 305–320.

Walker, D.L., Miles, L.A., and Davis, M. (2009). Selective participation of the bed nucleus of the stria terminalis and CRF in sustained anxiety-like versus phasic fear-like responses. Prog. Neuropsychopharmacol. Biol. Psychiatry *33*, 1291–1308.

Wang, L., Dankert, H., Perona, P., and Anderson, D.J. (2008). A common genetic target for environmental and heritable influences on aggressiveness in Drosophila. Proc. Natl. Acad. Sci. USA *105*, 5657–5663.

Weiss, I.C., Pryce, C.R., Jongen-Rêlo, A.L., Nanz-Bahr, N.I., and Feldon, J. (2004). Effect of social isolation on stress-related behavioural and neuroendocrine state in the rat. Behav. Brain Res. *152*, 279–295.

Wiberg, G.S., and Grice, H.C. (1963). Long-term isolation stress in rats. Science *142*, 507–508.

Witkin, J.M., Statnick, M.A., Rorick-Kehn, L.M., Pintar, J.E., Ansonoff, M., Chen, Y., Tucker, R.C., and Ciccocioppo, R. (2014). The biology of nociceptin/orphanin FQ (N/OFQ) related to obesity, stress, anxiety, mood, and drug dependence. Pharmacol. Ther. *141*, 283–299.

Yilmaz, M., and Meister, M. (2013). Rapid innate defensive responses of mice to looming visual stimuli. Curr. Biol. *23*, 2011–2015.

Zelikowsky, M., Hersman, S., Chawla, M.K., Barnes, C.A., and Fanselow, M.S. (2014). Neuronal ensembles in amygdala, hippocampus, and prefrontal cortex track differential components of contextual fear. J. Neurosci. *34*, 8462–8466.

STAR★METHODS

KEY RESOURCES TABLE

REAGENT or RESOURCE	SOURCE	IDENTIFIER
Antibodies		
Rabbit polyclonal anti-proNKB	Invitrogen	PA1-16745
Rabbit polyclonal anti-NeuN	Millipore	ABN78
Chicken polyclonal anti-PLP	Millipore	AB15454
Rabbit polyclonal anti-NFIA	Deneen B., Baylor	N/A
Goat anti-rabbit, Alexa Fluor 594	Invitrogen	R37117
Goat anti-chicken, Alexa Fluor 594	Invitrogen	A-11042
Bacterial and Virus Strains		
AAV2-EF1a-DIO-hM4D(Gi)-mCherry	UNC Vector Core	N/A
AAV2-EF1a-DIO-mCherry	UNC Vector Core	N/A
AAV1-CAG-FLEX-eGFP	UNC Vector Core	N/A
AAV5.H1.Tac2-shRNA1.CMV.ZsGreen.SV40	This paper	N/A
AAV5.H1.Tac2-shRNA2.CMV.ZsGreen.SV40	This paper	N/A
AAV5.H1.shRLuc.CMV.ZsGreen.SV40	This paper	N/A
AAVPHP.B-hSyn-Tac2-P2A-mCherry	This paper	N/A
AAVPHP.B-hSyn-Tac2-P2A-GFP	This paper	N/A
AAVPHP.B-hSyn-DIO-hM3D(Gq)-mCherry	This paper	N/A
AAVPHP.B -hSyn-DIO-mCherry	This paper	N/A
Chemicals, Peptides, and Recombinant Proteins		
DAPI	Sigma	D9542
Vectashield	Vector Labs	H-1000
Fluoro-Gel with Tris Buffer	Electron Microscopy Sciences	17985-10
Clozapine N-oxide	Enzo	NS105-0005
Osanetant	Axon	1533; SR 142801
Senktide	Tocris	1068
Digoxigenin-labeled Tac2 RNA probe	This paper	N/A
Digoxigenin-labeled Cfos RNA probe	This paper	N/A
Digoxigenin-labeled CRH RNA probe	This paper	N/A
DNP-labeled Tac2 RNA probe	This paper	N/A
DIG RNA Labeling Mix	Roche	11277073910
DNP-11-UTP	PerkinElmer	NEL555
T7 RNA Polymerase	Roche	10881767001
Anti-digoxigenin-POD	Roche	11207733910
Anti-DNP antibody, HRP conjugate	PerkinElmer	FP1129
Anti-DNP antibody, Alexa Fluor 488 conjugate	Invitrogen	A11097
Sheep serum	Sigma	S3772
TSA Blocking Reagent	PerkinElmer	FP1020
TSA Plus Biotin Kit	PerkinElmer	NEL749A001KT
TSA Plus DNP (HRP) kit	PerkinElmer	NEL747B001KT
Avidin/biotin blocking kit	Vector Labs	SP-2001
TSA Plus DNP (HRP) System	PerkinElmer	NEL747A001KT
Streptavidin Alexa Fluor 488 conjugate	Invitrogen	S11223
Streptavidin Alexa Fluor 594	Jackson ImmunoResearch	016-580-084
Proteinase K	NEB	P8107S

(*Continued on next page*)

Continued

REAGENT or RESOURCE	SOURCE	IDENTIFIER
Yeast tRNA	Sigma	R8759
Calf Thymus DNA	Invitrogen	15633019
Dextran sulfate	Sigma	D8906
Denhardt's Solution 50x	Sigma	D2532
PrimeSTAR Max DNA Polymerase	Takara	R045A
GeneArt Seamless Cloning and Assembly Kit	Invitrogen	A13288
RNAlater	QIAGEN	76106
RNAeasy Plus Mini Kit	QIAGEN	74134
TURBO DNase	Thermo Fisher	AM2238
Murine RNase Inhibitor	NEB	M0314L
Dynabeads MyOne Silane	Thermo Fisher	37002D
LightCycler 480 SYBR Green	Roche	4887352001
Superscript III Reverse Transcriptase	Life Technologies	18080093
Tac1 Primer	Integrated DNA Technologies	http://www.idtdna.com/pages
Tac2 Primer	Integrated DNA Technologies	http://www.idtdna.com/pages
GAPDH Primer	Integrated DNA Technologies	http://www.idtdna.com/pages
18 s Primer	Integrated DNA Technologies	http://www.idtdna.com/pages
Experimental Models: Organisms/Strains		
C57BL/6N	Charles River	N/A
BALB/c	Charles River	N/A
Tac2-Cre		N/A
Tac1-Cre		N/A
Ai6-zsGreen reporter	Madisen et al., 2010	N/A
Ai14-tdTomato reporter	Madisen et al., 2010	N/A
Recombinant DNA		
pAAV.H1.Tac2-shRNA1.CMV.ZsGreen.SV40	This paper	N/A
pAAV.H1.Tac2-shRNA2.CMV.ZsGreen.SV40	This paper	N/A
pAAV.H1.shRLuc.CMV.ZsGreen.SV40	U Penn Vector Core	PL-C-PV1781
pAAV-GFP	Cell Biolabs Inc	AAV-400
pAAV-hSyn-Tac2-P2A-mCherry	This paper	N/A
pAAV-hSyn-Tac2-P2A-GFP	This paper	N/A
pAAV-hSyn-DIO-hM3D(Gq)-mCherry	Addgene	44361
pAAV-hSyn-DIO-mCherry	Addgene	50459
Software and Algorithms		
ImageJ	NIH	https://imagej.nih.gov/ij
Prism 6	GraphPad Software	https://www.graphpad.com/
MATLAB	MathWorks	https://www.mathworks.com/
EthoVision XT	Noldus	http://www.noldus.com/
Looming Code, MATLAB	Meister M., Caltech	N/A
Behavior Annotator, MATLAB	Perona P., Caltech	N/A
Behavioral Analysis Code, MATLAB	This paper	N/A
Metamorph	Technical Instrument	http://www.techinst.com/
SiDirect 2.0	SiDirect 2.0	http://sidirect2.rnai.jp/
Other		
Cannulae (guide, dummy, internal)	Plastics One	N/A
Microinfusion Pump	Harvard Apparatus	https://www.harvardapparatus.com/

CONTACT FOR REAGENT AND RESOURCE SHARING

Further information and requests for reagents may be directed and will be fulfilled by the Lead Contact, David J. Anderson (wuwei@caltech.edu).

EXPERIMENTAL MODEL AND SUBJECT DETAILS

Animals

Wild-type (WT) C57BL/6N male mice (experimental), C57BL/6N female mice (for sexual experience), and BALB/c male mice (intruders) were obtained from Charles River (at 6-10 weeks of age). For visualization of Tac2 and Tac1 expression, we used previously described Cre-dependent Ai6-zsGreen and Ai14-tdTomato fluorescent reporter mice (Madisen et al., 2010), Tac2-IRES2-Cre (Cai et al., 2014), and Tac1-IRES2-Cre knockin mice (obtained from the Allen Institute for Brain Science), which were backcrossed to the C57BL/6N background in the Caltech animal facility. Tac2-IRES-Cre mice were used for Cre-dependent LOF/GOF experiments (Figures 5 and 7). Animals were housed and maintained on a reverse 12-hr light-dark cycle with food and water *ad libitum*. Behavior was tested during the dark cycle. Care and experimental manipulation of animals were in accordance with the National Institute of Health Guide for Care and Use of Laboratory Animals and approved by the Caltech Institutional Animal Care and Use Committee.

Social isolation stress

WT males (Charles River) were housed in isolation (1 animal per cage), or in groups of 3. Tac2-IRES-Cre males (bred in-house) were housed in isolation, or in groups of 2-5. Animals were isolated post-weaning, at 8-16 weeks of age. All cage conditions remained otherwise identical for group housed mice compared to isolated animals, and mice were housed on the same rack in the same vivarium. Except where otherwise indicated, social isolation was maintained for at least 2 weeks (this period was extended in the case of surgical experiments, i.e., when adequate time for recovery and viral expression levels were required). All mice were between 12-20 weeks of age at the time of behavioral testing.

METHOD DETAILS

Viral constructs

The AAV2-EF1a-DIO-hM4D(Gq)-mCherry and AAV2-EF1a-DIO-mCherry were acquired from the University of North Carolina (UNC) viral vector core. The pAAV-Tac2-shRNA1-CMV-zsGreen, pAAV-Tac2-shRNA2-CMV-zsGreen, and pAAV-shRLuc-CMV-zsGreen plasmids were constructed (see construction below) and serotyped with AAV5 coat proteins and packaged in-house (see viral packaging below). The pAAV-hSyn-Tac2-P2A-mCherry and pAAV-hSyn-Tac2-P2A-GFP plasmids were constructed (see below) and packaged into AAV-PHP.B (see PHP.B section below). The pAAV-hSyn-DIO-hM3D(Gq)-mCherry and pAAV-hSyn-DIO-mCherry were acquired from Addgene and packaged into AAV-PHP.B (see below).

Construction of small hairpin RNA expressing AAV vector

Small hairpin RNA (shRNA) for mouse Tac2 gene (NM_009312.2) were designed using the online designing tool siDirect 2.0 (http://sidirect2.rnai.jp/) (Naito et al., 2009). Oligonucleotides encoding Tac2 shRNAs were purchased from IDT. Oligonucleotides used were as follows: shRNA1, 5′- CCGACGTGGTTGAAGAGAACACCGCTTCCTGTCACGGTGTTCTCTTCAACCACGTCTTTTTT −3′ and 5′- AAAAAAGACGTGGTTGAAGAGAACACCGTGACAGGAAGCGGTGTTCTCTTCAACCACGTCGG −3′; shRNA2, 5′- CCGC CTCAACCCCATAGCAATTAGCTTCCTGTCACTAATTGCTATGGGGTTGAGGCTTTTTT −3′ and 5′- AAAAAAGCCTCAACCCCATAG CAATTAGTGACAGGAAGCTAATTGCTATGGGGTTGAGGCGG −3′

pAAV.H1.shRLuc.CMV.ZsGreen.SV40 (Luc shRNA) plasmid (PL-C-PV1781, Penn Vector Core) was used as shRNA AAV vector backbone and control shRNA construct. Entire Luc shRNA plasmid except luciferase shRNA sequence was amplified by PCR with the following primers: shRNA1, Forward - AACCACGTCTTTTTTAATTCTAGTTATTAATAGTAATCAA; Reverse - CTTCAA CCACGTCGGCTGGGAAAGAGTGGTCTC; shRNA2, Forward - GGTTGAGGCTTTTTTAATTCTAGTTATTAATAGTAATCAA ; Reverse - ATGGGGTTGAGGCGGCTGGGAAAGAGTGGTCTC. All PCR reactions were performed using PrimeSTAR Max DNA Polymerase (Takara Bio, Kusatsu, Japan). After PCR amplification, template plasmid was digested by DpnI (NEB, Ipswich, MA) and PCR amplicons were ligated with annealed shRNA oligoes using GeneArt Seamless Cloning and Assembly Kit (Thermo Fisher Scientific, Waltham, MA) following the manufacturer's instruction.

Construction of Tac2-overexpression AAV vectors

Tac2-P2A-mCherry gene fragment was synthesized in the form of IDT gBlocks (see below*). pAAV-hSyn-Tac2-P2A-mCherry was generated via ligation to AccI/NheI site of pAAV-hSyn-DIO-hM3D(Gq)-mCherry plasmid (Addgene #44361) using DNA Ligation Kit Mighty Mix (Takara Bio, Kusatsu, Japan). To generate pAAV-hSyn-Tac2-P2A-GFP plasmid, the entire pAAV-hSyn-Tac2-P2A-mCherry plasmid except the mCherry sequence was amplified by PCR with the following primers: Forward - CTCCTCGCCCTTGCTCAC; Reverse - GGCGCGCCATAACTTCGTATAATG and GFP sequence was amplified from pAAV-GFP plasmid (AAV-400, Cell Biolabs Inc, San Diego, CA) with the following primers: Forward - CCTGGACCTATGGTGAGCAAGGGCGAGGAGCTGTTCACCGGGGTGGTG;

Reverse - AGCATACATTATACGAAGTTATGGCGCGCCCTACTTGAGCTCGAGATCTGAGTAC. Both PCR amplicons were treated with DpnI (NEB) and ligated together using GeneArt Seamless Cloning and Assembly Kit (Thermo Fisher scientific) following the manufacture's instruction.

*Synthesized Tac2-P2A-mCherry gene fragment:

GCTAGCGCCACCATGAGGAGCGCCATGCTGTTTGCGGCTGTCCTCGCCCTCAGCTTGGCTTGGACCTTCGGGGCTGTGTGTG
AGGAGCCACAGGGGCAGGGAGGGAGGCTCAGTAAGGACTCTGATCTCTATCAGCTGCCTCCGTCCCTGCTTCGGAGACTCTAC
GACAGCCGCCCTGTCTCTCTGGAAGGATTGCTGAAAGTGCTGAGCAAGGCTTGCGTGGGACCAAAGGAGACATCACTTCCACAG
AAACGTGACATGCACGACTTCTTTGTGGGACTTATGGGCAAGAGGAACAGCCAACCAGACACTCCCACCGACGTGGTTGAAGAG
AACACCCCCAGCTTTGGCATCCTCAAAGGAAGCGGAGCTACTAACTTCAGCCTGCTGAAGCAGGCTGGAGACGTGGAGGAGAA
CCCTGGACCTATGGTGAGCAAGGGCGAGGAGGATAACATGGCCATCATCAAGGAGTTCATGCGCTTCAAGGTGCACATGGAGG
GCTCCGTGAACGGCCACGAGTTCGAGATCGAGGGCGAGGGCGAGGGCCGCCCCTACGAGGGCACCCAGACCGCCAAGCTGA
AGGTGACCAAGGGTGGCCCCCTGCCCTTCGCCTGGGACATCCTGTCCCCTCAGTTCATGTACGGCTCCAAGGCCTACGTGAAG
CACCCCGCCGACATCCCCGACTACTTGAAGCTGTCCTTCCCCGAGGGCTTCAAGTGGGAGCGCGTGATGAACTTCGAGGACGG
CGGCGTGGTGACCGTGACCCAGGACTCCTCCCTGCAGGACGGCGAGTTCATCTACAAGGTGAAGCTGCGCGGCACCAACTTC
CCCTCCGACGGCCCCGTAATGCAGAAGAAGACCATGGGCTGGGAGGCCTCCTCCGAGCGGATGTACCCCGAGGACGGCGCCC
TGAAGGGCGAGATCAAGCAGAGGCTGAAGCTGAAGGACGGCGGCCACTACGACGCTGAGGTCAAGACCACCTACAAGGCCAA
GAAGCCCGTGCAGCTGCCCGGCGCCTACAACGTCAACATCAAGTTGGACATCACCTCCCACAACGAGGACTACACCATCGTGG
AACAGTACGAACGCGCCGAGGGCCGCCACTCCACCGGCGGCATGGACGAGCTGTACAAGTAAGGCGCGCCATAACTTCGTATA
ATGTATGCTATACGAAGTTATTAAGAGGTTTCATATTGCTAATAGCAGCTACAATCCAGCTACCATTCTGCATAACTTCGTATAAAG
TATCCTATACGAAGTTATTCCGGAGTCGAC

Viral packaging

rAAVs were produced by polyethylenimine (PEI) triple transfection of HEK293T cells. Briefly, 40μg of equi-molar pHelper, pXR5 and pAAV-trans DNA plasmids were mixed with 120μl of 1mg/ml Polyethylenimine HCl MAX (Polysciences) in PBS and incubated at RT for 5 minutes. 90% confluent HEK293 cells grown on 15cm tissue culture plates were transfected with the plasmid/PEI mixture. Cells were collected 72 hours post transfection, freeze-thawed 3 timed and incubated with Benzonase (Millipore) at 5 units/mL for 1 hour. The solution was then centrifuged at 5000xg for 20 minutes. The supernatant was layered on top of a discontinuous gradient of iodixanol and centrifuged at 200,000xg for 2 hours at 18°C. The 40% iodixanol fraction was collected, concentrated, and buffer exchanged with PBS using a Millipore 100kD centrifugal filter. AAV genomic titers were determined by real-time PCR using primers against the ITR and normalized by dilution with PBS to $1x10^{12}$ genome copies per mL virus.

AAV-PHP.B production and intravenous administration

The AAV-hSyn-DIO-Tac2-P2A-mCherry, AAV-hSyn-DIO-Tac2-P2A-GFP, AAV-hSyn-DIO-hM3D-mCherry, and AAV-hSyn-DIO-mCherry recombinant AAV genomes were separately packaged into the AAV-PHP.B capsid by triple transfection of HEK293T cells and purified with iodixanol step gradients as previously described (Deverman et al., 2016). $5x10^{11}$ vector genomes (vg) of each virus was administered intravenously (via the retro-orbital sinus) to Tac2-Cre animals individually, or in combination. To equalize the amount of virus given to each mouse, $5x10^{11}$ vg of AAV-PHP.B-hSyn-DIO-mCherry was administered to each animal to bring them up to the amount injected in the double Tac2+hM3DREAAD group. Each animal received a total vector dose of $1x10^{12}$ vg.

Surgery and cannula implants

Mice 8-16 weeks old were anesthetized with isoflurane and mounted in a stereotaxic apparatus (Kopf Instruments). Anesthesia was maintained throughout surgery at 1%–1.5% isoflurane. The skull was exposed and small burr holes produced dorsal to each injection site using a stereotaxic mounted drill. Virus was backfilled into pulled fine glass capillaries (~50 μm diameter at tip) and pressure injections of 300nl were made bilaterally into either the dBNSTa (AP +0.25, ML ± 0.85, DV −4.1), DMH (AP −1.3, ML ± 0.35, DV −5.6), or CeA (AP −1.4, ML ± 2.6, DV −4.73) at a rate of 30nl per minute using a nanoliter injector (Nanoliter 2000, World Precision Instruments) controlled by an ultra microsyringe pump (Micro4, World Precision Instruments). Capillaries remained in place for 5 minutes following injections to allow for full diffusion of virus and to reduce backflow up the injection tract. Skin above the skull was then drawn together and sealed with GLUture (Zoetis). For bilateral cannula implantations, single or double guide cannula (custom, Plastics One) aimed 0.5mm above each region were implanted and held in place with dental cement (Parkell). Compatible dummy cannulas with a 0.5mm protrusion at the tip were inserted to prevent cannula clogging. Directly following surgery, mice were given a subcutaneous injection of ketoprofen (2mg/kg) and supplied with drinking water containing 400mg/L sulphamethoxazole and 200mg/L ibuprofen and monitored for 7 days. Dummies were replaced every 2-3 days to keep cannula tracts clean. All injections were subsequently verified histologically.

Immunohistochemistry

Immunofluorescence staining proceeded as previously described (Anthony et al., 2014; Cai et al., 2014; Hong et al., 2014; Kunwar et al., 2015). Briefly, mice were perfused transcardially with 0.9% saline followed by 4% paraformaldehyde (PFA) in 1XPBS. Brains were extracted and post-fixed in 4% PFA overnight at 4°C followed by 48 hours in 15% sucrose. Brains were embedded in OCT

mounting medium, frozen on dry ice, and stored at −80°C for subsequent sectioning. Sections 40-50 μm thick were cut on a cryostat (Leica Biosystems). Sections were either directly mounted onto Superfrost slides for histological verification of injections/cannula placements or were cut free floating for antibody staining. For antibody staining, brain sections were washed 3X in 1XPBS and blocked in PBS-T (0.3% Triton X-100 in 1XPBS) with 10% normal goat or donkey serum for 1hr at room temperature (RT). Sections were then incubated in primary antibody diluted in blocking solution at 4°C for 48-72 hours. We stained for neurokinin B (rabbit anti-proNKB; 1:1000; Invitrogen); the glial marker nuclear factor I-A (rabbit anti-mouse NFIA; 1:1000; Deneen lab) (Deneen et al., 2006); the oligodendrocyte marker proteolipid protein (chicken anti-PLP; 1:1,000; Millipore) or the nuclear marker NeuN (rabbit anti-NeuN; 1:1000; Millipore). Sections were then washed 3X and incubated in secondary antibodies diluted in blocking buffer (goat anti-rabbit, goat anti-chicken, Alexa Fluor 594, 1:500) overnight at 4°C. Sections were then washed 3X, incubated for 20 minutes at RT in DAPI diluted in 1XPBS (1:2000) for counterstaining, washed again, mounted on Superfrost slides, and coverslipped for imaging on a confocal microscope (Olympus FluoView FV1000).

Fluorescent *in situ* hybridization

Digoxigenin (DIG)-labeled *Tac2, Cfos, Crh* RNA probes and dinitrophenyl (DNP)-labeled *Tac2* probe were generated following a previously described protocol (http://help.brain-map.org/display/mousebrain/Documentation) (Lein et al., 2007) with the following primer sets: Tac2; Forward - AGCCAGCTCCCTGATCCT; Reverse - TTGCTATGGGGTTGAGGC (NM_009312.2, 36-608bp *Cfos*; Forward - agaatccgaagggaacgg and Reverse - ggaggccagatgtggatg (NM_010234.2, 560-1464bp) *Crh*; Forward - agggaggagaagagagc and Reverse agccacccctcaagaatg (NM_205769.3, 219-1185bp). Fluorescent *in situ* hybridization (FISH) or double fluorescent *in situ* hybridization (dFISH) was carried out according to the protocol used in (Thompson et al., 2008) with modifications. Briefly, mice were transcardially perfused with 1 x PBS followed by 4% paraformaldehyde/PBS (PFA) in 1 x PBS. Brains were fixed in 4% PFA 3-4 hours at 4°C and cryoprotected for overnight in 15% sucrose at 4°C. Brains were embedded in OCT Compound (Fisher Scientific) and cryosectioned in 30 μm thickness and mounted on Superfrost Plus slides (Fisher Scientific). Sections were fixed in 4% PFA for 30 min, acetylated with 0.25% acetic anhydride in 0.1 M triethanolamine for 10 min, dehydrated with increasing concentrations of EtOH (50, 70, 95 and 100%), gently treated with proteinase K (6.3 μg/mL in 0.01M Tris-HCl pH7.4 and 0.001M EDTA) for 10 min, and fixed in 4% PFA for 20 min. All procedures were performed at room temperature (RT). The hybridization buffer contained 50% deionized formamide, 3 × standard saline citrate (SSC), 0.12 M PB (pH 7.4), 10% dextran sulfate, 0.12 mg/ml yeast tRNA, 0.1 mg/mL calf thymus DNA, and 1x Dehardt solution. The sections were prehybridized at 63°C in hybridization buffer for 30 min and then hybridized with RNA probes (300ng/ml for each probe) in hybridization buffer at 63°C for 16 hours. After hybridization, the sections were washed with 5 × SSC for 10 min, 4x SSC / 50% formamide for 20 min, 2x SSC / 50% formamide for 30min, and 0.1x SSC for 20min twice each at 61°C. The sections were blocked with 4% sheep serum in TNT buffer (Tris-HCl pH7.5, 0.15 M NaCl and 0.00075% tween 20) for 30 min and TNB Blocking buffer (TSA blocking reagent, PerkinElmer, Waltham, MA) for 30 min at RT. The sections were incubated with anti-digoxigenin-POD antibody (1:600, Roche Diagnostics) in TNB buffer overnight at RT. The sections were washed with TNT buffer and tyramide-biotin signal amplification was performed using the TSA Plus Biotin Kit (PerkinElmer) and signals were visualized after 1 hr incubation with Alexa Fluor 594 Streptavidin (Jackson ImmunoResearch) or Alexa Fluor 488 Streptavidin (Invitrogen) at RT. The sections were washed with TNT buffer and fixed with 4% PFA for 20 min at RT, washed with PBS, blocked with avidin/biotin blocking kit (Vector), and then treated with 0.3% H_2O_2 for 15 min at RT. Subsequently, the sections were washed with PBS, blocked with TNB blocking buffer for 20 min at RT, and incubated with anti-DNP HRP conjugated antibody (1:250, PerkinElmer) in TNB blocking buffer overnight at RT. On the following day, the sections were washed with TNT buffer and tyramide-DNP signal amplification was performed using the TSA Plus DNP (HRP) Kit (PerkinElmer) and signals were visualized with Anti-DNP Alexa Fluor 488 conjugated antibody (1:125, Invitrogen) at RT. Sections were counterstained with DAPI (0.5ug/mL in PBS), washed with 1 x PBS, and coverslipped using Fluoro-Gel with Tris Buffer (Electron Microscopy Sciences). Tissue images of entire coronal brain sections were taken using a slide-scanner (VS120-S6-W, Olympus) or a confocal microscope (FluoView FV1000, Olympus) and cells positive for the probes were counted as described below.

Cell counting

Following confocal or slide-scanner imaging, quantification of labeled cells was performed using ImageJ and Metamorph. Cells were counted by an observer blind to experimental conditions. Brain images were converted to greyscale (16-bit) in ImageJ and adjusted using automatic thresholding and watershed separation. Cells were either counted automatically using ImageJ's particle analysis algorithm (random sections were counted manually to cross-check that automated scoring was consistent with manual human scoring); otherwise, cells were counted manually using MetaMorph. Cells that were not entirely contained within a given region of interest (ROI) were excluded from analyses. Relative fluorescent intensities (for cell body or projection terminal labeling with a fluorescent protein) were measured automatically using MetaMorph for a given ROI. Raw cell counts within an ROI were divided by the size of the ROI (mm^2) to produce the number of positively labeled cells/mm^2.

Quantitative real-time reverse transcription PCR

Group housed or isolated (30 minutes, 24 hours, 2 weeks) mice were decapitated and brains were quickly removed and placed in RNA Later (QIAGEN) at 4°C. Tissue from dBNSTa, DMH, CeA, ACC, and dHPC was micro-dissected and placed in RNA Later. Tissue was

then homogenized and RNA purified using an RNAeasy Plus Mini Kit (QIAGEN). 150ng of total RNA/region/condition was then incubated with 3μl of Turbo DNase, 1μl of Murine RNase Inhibitor, in 1X Turbo DNase buffer for 15 minutes at 37°C to remove any contaminating genomic DNA. Samples were subsequently purified using Dynabeads MyOne Silane beads and eluted in 11 μl. The eluted RNA was used as input into a 20μl reverse transcriptase reaction (SuperScript III). 1μl of 100μM random 9mers (NNNNNNNNN - IDT corporation) served as primers. The reverse transcriptase reaction was inactivated at 70°C prior to qPCR analysis on the LightCycler 480 Instrument II. The following primers, ordered from Integrated DNA Technologies, were used: Tac1 (Forward – GATGAA GGAGCTGTCCAAGC; Reverse – TCACGAAACAGGAAACATGC); Tac2 (Forward– GCCATGCTGTTTGCGGCTG; Reverse – CCTTG CTCAGCACTTTCAGC); GAPDH (Forward –TGAAGCAGGCATCTGAGGG; Reverse – CGAAGGTGGAAGAGTGGGAG); and 18 s (Forward – GCAATTATTCCCCATGAACG; Reverse – GGGACTTAATCAACGCAAGC). GAPDH and 18S ribosomal RNA served as housekeeping genes to which Tac1 and Tac2 were normalized. Primers were resuspended in ddH20 to 100μM. A 25μM mix of each primer was used as input for qRT-PCR reaction. Four technical replicates were run for each sample primer pair and the Cp (Crossing Point) value was determined using Lightcycler II Software. The median value of the four technical replicates was used as the representative value for the set. Final mRNA fold increase values were determined by normalizing raw fluorescent values of experimental animals to controls using the following formula: $2^{\wedge(\text{Cycles Control - Cycles Experimental})}$. Thus for example, if the control sample required 8 cycles and the experimental sample 3 cycles to reach the Cp, then the fold-increase for experimental/control would be $2^{(8-3)} = 2^5 = 32$-fold.

Resident intruder assay

Testing for aggression using the resident intruder assay (Blanchard et al., 2003) proceeded as previously described (Hong et al., 2014, 2015; Lee et al., 2014). Briefly, experimental mice (“residents”) were transported in their homecage to a novel behavior testing room (cagemates in group housed mice were removed from the homecage prior to transport for this and all other behavioral tests), where they acclimated for 5-15 minutes. Homecages were then slotted into a customized behavioral chamber lit with a surround panel of infrared lights and equipped with two synchronized infrared video cameras (Pointgrey) placed at 90-degree angles from each other to allow for simultaneous behavior recording with a front and top view. Synchronized video was acquired using Hunter 4.0 software (custom, Pietro Perona lab, Caltech). Following a two-minute baseline period, an unfamiliar male BALB/c mouse (“intruder”) was placed in the homecage of the resident for 10 minutes and mice were allowed to freely interact. Group housed BALB/c males were used as intruders because they are a relatively submissive strain, thereby reducing any intruder initiated fighting. Behavior videos were hand annotated by an observer blind to experimental conditions (Behavior Annotator, Piotr’s MATLAB toolbox; https://pdollar.github.io/toolbox/). Fighting bouts were scored on a frame-by-frame basis and were defined as a frame in which the resident male was currently engaged in an episode of biting or intense aggressive behavior immediately surrounding a biting episode. Annotation files were then batch analyzed for behavior, including number of fighting bouts, using in-house customized programs in MATLAB (A. Kennedy, Caltech).

Looming disk assay

Freezing behavior to presentation of an overhead looming disk proceeded as previously described (Kunwar et al., 2015; Yilmaz and Meister, 2013). Briefly, mice were transported to a novel behavioral testing room. After 5 minutes of acclimation, mice were placed inside a novel, custom-built open top Plexiglas arena (48 × 48 × 30 cm) covered with a flat screen monitor placed directly above and illumination provided by infrared LEDs (Marubeni). Mice were given a 5 minute baseline period in the arena, following which entry into the center of the arena triggered presentation of a single, 10 s overhead looming disk stimulus (comprised of a single looming disk presentation 0.5 s in duration, which was repeated 10 times with an inter-stimulus interval of 0.5 s). The stimulus was controlled by custom MATLAB code (M. Meister, Caltech) run on dedicated computer in an adjacent room. Mice remained in the area for an additional 2 minutes before being transported back. Behavior was recorded using a video recorder attached to a laptop equipped with video capture software (Corel VideoStudio Pro). Acute freezing behavior to the looming disk (“during”), as well as in the 30 s following the last disk (“post”) were scored manually (Behavior Annotator, MATLAB) by an observer blind to environmental conditions.

Tone fear conditioning and shock reactivity

The protocol for tone trace fear conditioning occurred as previously described (Cushman et al., 2014) in fear conditioning boxes previously described in detail (Haubensak et al., 2010; Kunwar et al., 2015). Briefly, mice were transported in squads of four on a white cart to a novel behavioral testing room containing 4, sound-attenuating fear-conditioning chambers (Med Associates). This “training context” was comprised of flat grid flooring (wired to a shock generator and scrambler for footshock delivery, Med Associates), houselights, and the presence of an internal fan for background noise. Chambers were sprayed with a 70% Simple Green solution on the underlying chamber pan to generate a unique contextual scent and chambers were cleaned with 70% EtOH between squads. Trace fear conditioning consisted of a 3 minute baseline period followed by 3 tone-shock trials consisting of a 20 s tone conditional stimulus (CS; 75dB, 2800 Hz), a 20 s trace interval and a 2 s footshock unconditional stimulus (US; 0.7mA). The inter-trial interval (ITI) between trials was 60 s. Mice remained in the chambers an additional 60 s before transport back to the vivarium. The following day, mice were transported in fresh cardboard boxes to a novel behavioral testing room consisting of 4 distinct fear-conditioning boxes to test for tone fear. The “test context” consisted of the houselights and fan turned off, uneven grid flooring, a 1% acetic acid scent and

a black plastic insert used to generate a triangular roof. Testing occurred identical to training with the exception that shocks were omitted from test trials to allow for behavior assessment to the tone. A single shock was administered in the last minute of testing to assess activity burst responding to the shock. This allowed us to assess reactivity to the shock under our various manipulations performed at test without disrupting fear acquisition by performing manipulations during training. All experimental manipulations and data displayed in the manuscript were performed during the test phase of fear conditioning (training data not shown). Training and testing context were counterbalanced across mice. Freezing behavior during the baseline period as well as during each tone presentation ("during") and trace interval ("post") were assessed as previously described (Zelikowsky et al., 2014) using automated near-infrared video tracking equipment and computer software (VideoFreeze, Med Associates). Shock reactivity (motion, arbitrary units) was measured during the 2 s shock US as well as the 3 s immediately following. Acute footshock stress (Figures S3L–S3M) was generated by delivering 4 unsignaled administrations of a 2 s, 0.7mA footshock following a 3 minute baseline period. The ITI was 90 s.

Ultrasonic sound stimulus assay

Behavior was tested as previously described (Mongeau et al., 2003). Briefly, mice were brought into a novel experimental testing room in their homecages and allowed to acclimate for 5 minutes. Behavior in the homecage to an ultrasonic sound stimulus (USS) was then recorded using a digital video camera connected to a portable laptop equipped with video capture software (Corel VideoStudio Pro). Mice received a two-minute baseline period behavior followed by three, 1 minute presentations of the USS (100ms frequency sweeps between 17 and 20 kHz, 85 dB, alternately ON 2 s/OFF 2 s) with a 1-minute inter-trial interval. Following testing mice were returned to the vivarium. Freezing behavior to each USS and post-USS period (ITI) was manually scored by an observer blind to experimental conditions (Behavior Annotator, MATLAB).

Open field test

Open field testing (OFT) occurred as previously described (Anthony et al., 2014; Cai et al., 2014; Kunwar et al., 2015) to examine anxiety-like behavior (thigmotaxis) in a novel open arena. Briefly, mice were brought into a novel behavior testing room in squads of 4. They were then individually placed in plastic open top arenas (50 X 50 X30cm) and allowed to freely move for a 10 minute period. Video was captured using an overhead mounted video camera connected to a dedicated computer in an adjacent room equipped with Mediacruise (Canopus) video capture software. Ethovision software was used to generate trajectory maps and analyze time spent in the center of the arena (center 50%) and average velocity.

Elevated plus maze

Elevated plus maze (EPM) testing occurred as previously described (Cai et al., 2014; Kunwar et al., 2015). Briefly, mice were brought into a behavioral testing room and tested for anxiety-like behavior on an elevated plus maze. The EPM was comprised of a platform (74cm above the floor) with four arms – two opposing open arms (30 × 5cm) and two opposing closed arms (30 × 5 × 14cm). Mice were placed in the center of the EPM and their behavior was tracked for 5 minutes using Mediacruise (Canopus) for video capture and Ethovision for trajectory maps, analyses of time spent in each arm, and number of entries. Mice were also scored for whether or not they jumped off of the center of the platform within 5 s of being initially placed on the EPM.

Acoustic startle response

Startle responding to an acoustic stimulus (Koch, 1999) was measured using a startle chamber (SR-LAB; San Diego Instruments) as previously described (Shi et al., 2003). Briefly, mice (in squads of 3) were brought into a novel behavioral testing room in their homecages and allowed to acclimate for 5 −10 minutes. Mice were then placed into sound-attenuating startle chambers comprised of a Plexiglas cylinder (5.1cm diameter) mounted on a platform (20.4 × 12.7 × 0.4 cm) with a piezoelectric accelerometer unit attached below to detect startle motion. The chambers contained an overhead loudspeaker and light. Following a 3 minute baseline, mice were presented with a series of 8 noise presentations ramping up from 67-124dB (67, 78, 86, 95, 104, 109, 115, 124dB) across a 4 minute period (~30 s variable inter-trial interval; ITI). The delivery of acoustic stimuli and acquisition of startle motion was controlled by SR-LAB software on a dedicated computer. Prior to each behavioral testing session, sound levels were calibrated with a sound-level meter (Radio Shack), and response sensitivities were calibrated using the SR-LAB Startle Calibration System. Startle chambers were cleaned with 70% EtOH between squads.

Flinch-vocalize-jump assay

Sensitivity to a noxious footshock stimulus was assessed using the flinch-vocalize-jump assay (Kim et al., 1991). Mice were transported to a behavioral testing room and individually tested in a fear conditioning box (Med Associates) for reactivity to a series of manually delivered shocks ramping up in amplitude. Shocks were administered every 5 s beginning from 0.05 mA until 0.6 mA, with each shock increasing by 0.05 mA. The shock intensity level at which the mouse displayed flinching (first perceptible reaction to the shock), vocalization (sound audible to a human observer), and jumping (simultaneous lifting of all 4 paws off the grid) was noted for each mouse.

Social interaction assay

Mice were tested for interactive behavior toward a novel mouse using the social interaction assay. Behavior proceeded as previously described (Hsiao et al., 2013). Briefly, mice were brought to a behavioral testing room in squads of 4 and individually placed in a long Plexiglass apparatus (50 × 75 cm) consisting of three chambers – a center chamber and two side chambers each containing an empty pencil cup flipped upside-down. Following a 5 minute baseline period, an unfamiliar male mouse (BALB/c) was placed under one pencil cup, and a novel object (50 mL falcon tube cut in half) was placed under the other (placements counterbalanced across mice). Sociability across a 10 minute time period was assessed. Video was captured using an overhead mounted video camera connected to a dedicated computer in an adjacent room equipped with Mediacruise (Canopus) video capture software. Ethovision software (Noldus) was used to analyze time spent in each chamber and generate an output file containing information on XY coordinates (location). XY coordinates were then used to generate heatmaps reflecting the amount of time spent at each location in the social interaction apparatus (MATLAB).

Rat exposure assay

Behavior was tested as previously described in Kunwar et al. (2015). Briefly, mice were tested for behavior toward an intact rat predator (Blanchard et al., 2005) weighing 300–500 g. Mice were brought in their homecage into a novel testing environment. Behavior was recorded using a digital video camera attached to a portable laptop running video acquisition software (Corel VideoStudio Pro). Following a 3 minute baseline period, a rat was lowered onto one side of the mouse's homecage in a custom-made mesh enclosure (16 × 11 × 15 cm) for a 5 minute time period. In order to assess where the mouse spent its time, the home cage was divided into three equal zones with Zone 1 being closest to the rat and Zone 3 farthest. Time spent in each zone as well freezing behavior (not shown) was calculated using EthovisionXT software (Noldus).

Pharmacology

Mice were administered the Nk3R antagonist osanetant (Axon Medchem, Axon 1533) either systemically or intra-brain region. Osanetant was dissolved in saline with 0.1% Tween 20 (vehicle). For systemic administration mice received an intraperitoneal (i.p.) injection (5 mg/kg) 20 minutes prior to behavioral testing. For microinfusions, guide cannula were removed from mice and replaced with injector cannula (Plastics One), which protruded 0.5mm from the tip of the guide cannula. Injectors were attached to 5 μL Hamilton syringes with PE tubing (Plastics One) and mounted on a microinfusion pump (Harvard Apparatus) for controlled bilateral infusion of osanetant (0.3 μL vehicle with 375 ng dose per site injected across 6 minutes). In a separate experiment, mice were administered the Nk3R agonist, Senktide (Tocris, 1068). Senktide was dissolved in saline and injected i.p. (2mg/kg) 20 minutes prior to behavioral testing. For experiments using systemic administration of clozapine-N-oxide (CNO), CNO (Enzo Life Sciences-Biomol, BML-NS105-0005) was dissolved in saline (9 g/L NaCl) and injected (i.p.) at 5 mg/kg for hM4DREADD silencing or 2 mg/kg for hM3DREADD activation 20 minutes prior to behavioral testing. CNO was also administered chronically in drinking water (0.5mg CNO/100ml water).

QUANTIFICATION AND STATISTICAL ANALYSIS

All behavioral data was scored by a trained observer blind to experimental conditions, or scored using an automated system (Ethovision, Med Associates). Data were then processed and analyzed using MATLAB, Excel, Prism 6, and G*Power. Statistical analyses were conducted using ANOVAs followed by Bonferroni post hoc tests, Fisher's LSD tests, and unpaired t tests when appropriate. The n value, the mean values ± SEM for each dataset, and statistically significant effects are reported in each figure/figure legend. The significance threshold was held at $\alpha = 0.05$, two-tailed (not significant, ns, $p > 0.05$; *$p < 0.05$; **$p < 0.01$; ***$p < 0.001$). Full statistical analyses corresponding to each dataset, including 95% confidence intervals (CIs) and effect size (η^2), are presented in Table S1.

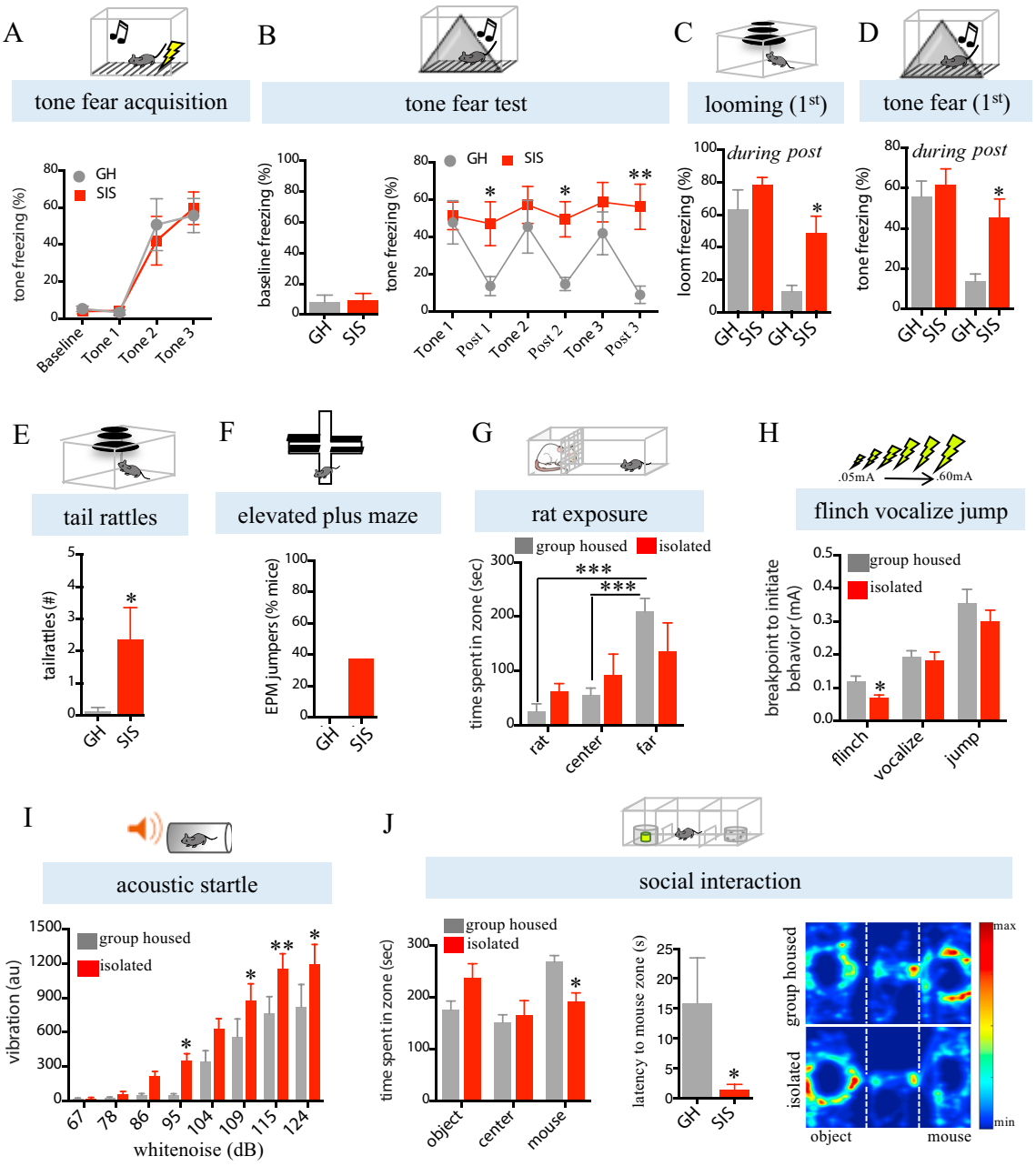

Figure S1. Prolonged SIS Alters Subsequent Social and Asocial Behavior, Related to Figure 1

(A) SIS or GH mice (n = 8 mice/condition) were tested in various behavioral assays (see Figure 1E). Tone fear acquisition curves showing baseline freezing to the conditioning context averaged across three minutes followed by freezing to each of three tones (30 s) prior to shock administration. Acquisition rate and final asymptotic values were not different between housing conditions.

(B) Left panel, baseline freezing to the tone fear test context averaged across the three minutes of context exposure prior to the initial tone (related tone test data presented in Figure 1H). No significant generalized freezing to the test context in either group was observed. Right panel, breakdown of freezing to each tone (30 s, "during") and each trace interval (20 s, "post"). Freezing in SIS mice persisted into each trace interval (see Figure 1H for averaged values).

(C) A novel, naive cohort of SIS or GH mice (n = 5-6 mice/condition) were tested on the looming disk assay without any prior behavior testing to control for order effects of testing after the resident intruder assay (see Figure 1E). SIS mice froze significantly more during the post period following presentation of the looming disk.

(D) A novel, naive cohort of SIS or GH mice (n = 8 mice/condition) underwent tone fear conditioning without any prior behavior testing to control for order effects of testing after the resident intruder and looming disk assays (see Figure 1E). SIS mice froze significantly more during the post period following presentation of the tone.

(E) Tail rattles during the overhead looming disk assay were elevated in isolated mice (see Figure 1G for looming data).

(legend continued on next page)

(F) The percent of mice that jumped off of the EPM within 5 s of initial placement in the center of the maze. EPM open versus closed-arm time data presented in Figure 1N.

(G) Mice that had been tested on the USS assay (Figure 1J) were tested in a rat exposure assay. GH mice spent significantly more time in the zone farthest away from the rat compared to the other zones. This preference for the "far" zone was absent in SIS mice.

(H and I) SIS or GH mice (n = 8 mice/condition) were tested in the flinch-vocalization-jump assay (H) and the acoustic startle assay (I) to measure reactivity to noxious stimuli presented at varying intensities. SIS mice showed flinch responding to footshocks of a lower magnitude (milliamp, mA) compared to GH mice (H). Startle responding to a white noise auditory stimulus was enhanced in SIS animals, even at sound decibel (dB) intensities that were sub-threshold for eliciting startle (I).

(J) SIS or GH mice (n = 8 mice/condition) were tested in the social interaction assay. SIS mice spent significantly less time in the zone containing a novel naive mouse in a pencil cup (left graph), but showed a shorter latency to initially enter the zone containing the mouse (right graph). Representative heatmaps (right panels) reflecting time spent in each location of the interaction apparatus (red, maximum time; dark blue, minimum time) for a GH (top) or SIS (bottom) mouse. In this and in all subsequent figures, *$p < 0.05$, **$p < 0.01$, ***$p < 0.001$. Bars without asterisks did not reach significance ($p > 0.05$). ANOVA's, *F's*, and *t* values as well as additional statistical information for this and subsequent supplemental figures can be found in Table S1. Data are represented as mean ± SEM.

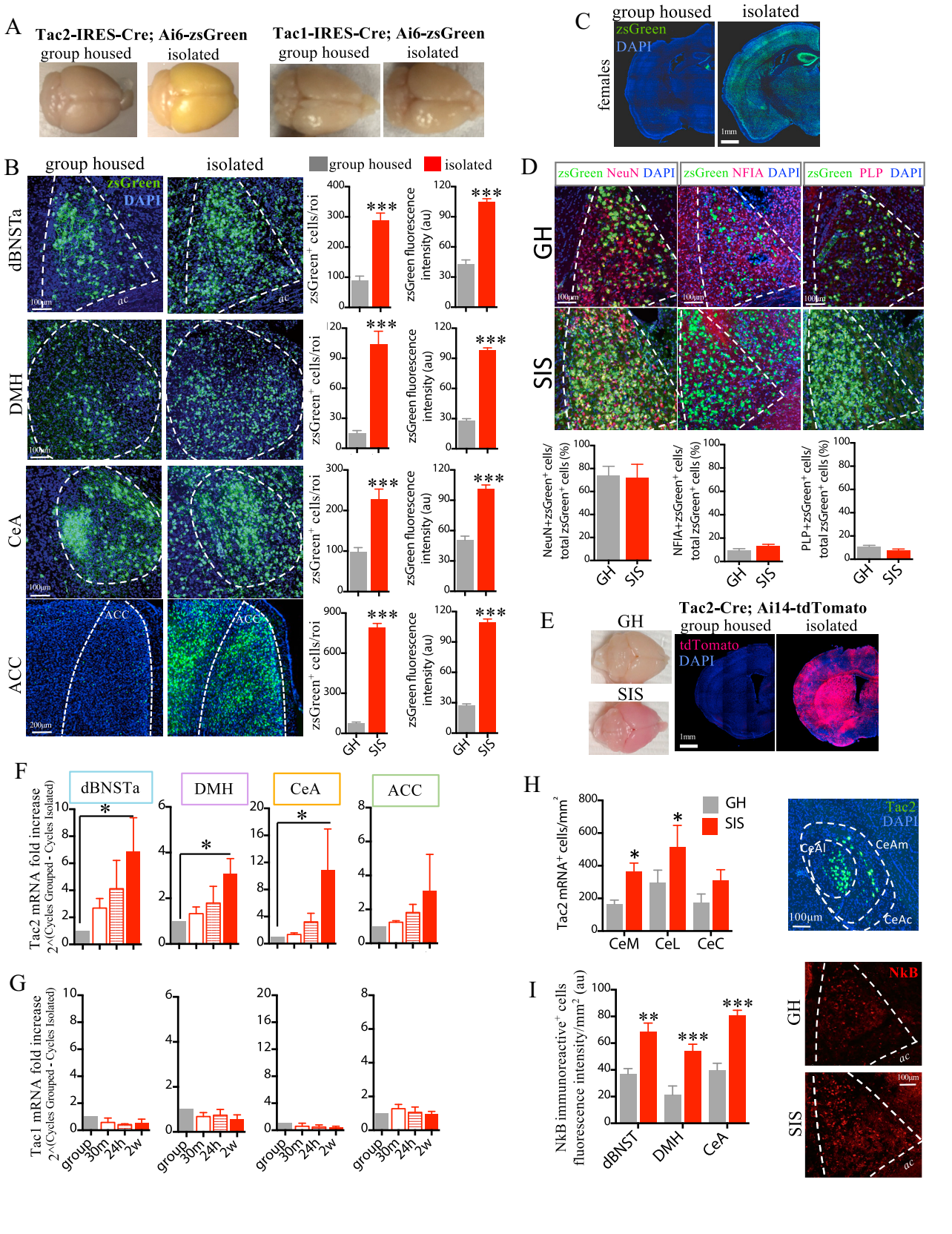

(legend on next page)

Figure S2. SIS Produces an Increase in Tac2 Expression, Related to Figure 2

(A) Tac2-IRES-Cre and Tac1-IRES-Cre mice were crossed to Ai6-zsGreen reporter mice (see Figures 2C and 2D). Whole, intact brains photographed under ambient lighting show increased zsGreen fluorescence present in isolated Tac2-IRES-Cre; Ai6-zsGreen mice (left panels) but not isolated Tac1-IRES-Cre; Ai6-zsGreen mice (right panels) or group housed mice.

(B) Representative coronal sections through dBNSTa, DMH, CeA, and ACC (top to bottom) illustrating Tac2-dependent zsGreen expression in GH (left panels) versus SIS mice (right panels). Quantification of zsGreen$^+$ cell counts (left) and average fluorescence (right) are presented alongside each respective region. Counts/fluorescence were restricted to each region as outlined (white dashed line). SIS produced significant increases in zsGreen expression across regions.

(C) Coronal images of Tac2-IRES-Cre; Ai6-zsGreen female mice illustrating that zsGreen expression is increased in females as well as in males.

(D) ZsGreen$^+$ cells in the dBNSTa co-labeled with the neuronal marker NeuN, the glial marker nuclear factor I-A (NFIA) and the oligodendrocyte marker proteolipid protein (PLP) (left to right). Coronal sections and percentage of zsGreen$^+$ cells that are double labeled with each respective marker in GH (top) compared to SIS mice (bottom) (n = 2-4 mice/condition; 3-4 sections/mouse). Upregulation of Tac2/zsGreen occurred preferentially in neurons.

(E) Tac2-IRES-Cre mice were crossed to Ai14-tdTomato reporter mice and group housed or isolated to confirm that the SIS-induced increase in zsGreen expression was not an artifact due to the reporter mouse (n = 4 mice/condition). Representative coronal sections illustrating increased Tac2-tdTomato expression.

(F and G) Mice were group housed or isolated for 2 weeks, 24 hr, or 30 minutes (n = 4 mice/condition), and tissue for each indicated region was dissected and processed for qRT-PCR analyses. Quantification of fold increases in Tac2 (F) or Tac1 (G) mRNA revealed significant increases in Tac2, but not Tac1, following 2 weeks of SIS. Data from the GH versus 2 week condition are also presented in Figures 2E and 2F and are included here for comparison purposes.

(H) Breakdown of expression of Tac2 mRNA in the different sub-compartments of CeA including the medial (CeM), lateral (CeL), and central (CeC) sub-divisions (n = 3-4 mice/condition; 3-4 sections/mouse). SIS mice showed a significant increase in Tac2 mRNA expression in both the CeM and CeL subregions (counts, left panel; representative image of SIS mouse, right panel). Data related to Figures 2I–2N.

(I) Neurokinin B (NkB) immunoreactivity in dBNSTa, DMH and CeA following 2 weeks of SIS compared to GH mice (n = 3 mice/condition, 1-2 sections/mouse). Representative confocal image of NkB expression in the dBNSTa (right) and quantification of average fluorescence intensity per mm^2 within each region (left) show elevated NkB protein expression in SIS mice.

BLA, basolateral amygdala. AC, anterior commissure.

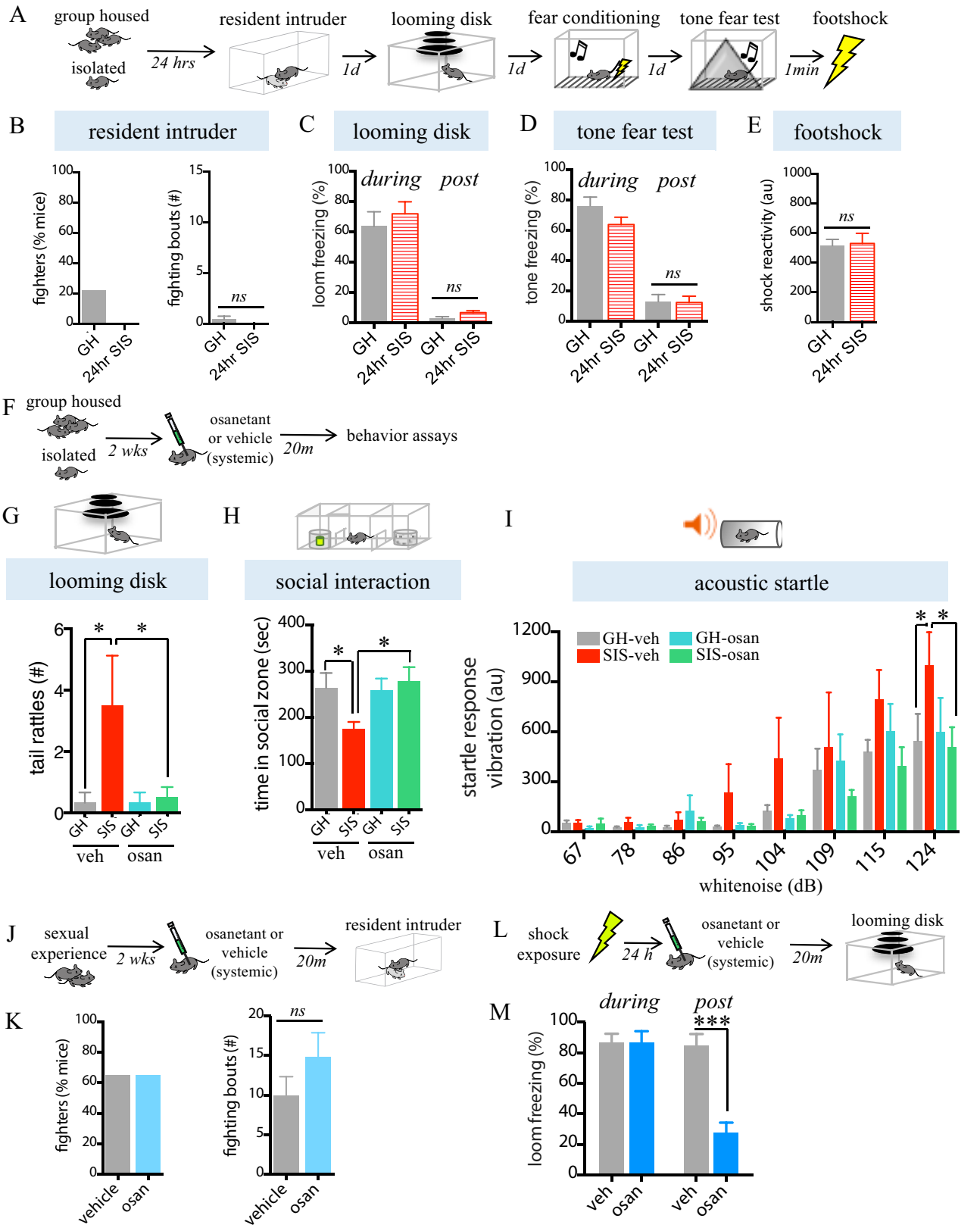

(legend on next page)

Figure S3. Effects of Systemic Acute Osanetant on Behavior, Related to Figure 3

(A) Experimental protocol for B-E. Mice were group housed or isolated for 24 hr and tested in indicated behavioral assays.

(B–E) There was no significant difference between GH mice and mice isolated for 24 hr on any of the assays tested.

(F) Experimental protocol for G-I. Mice were group housed or isolated for 2 weeks and tested on the indicated behavioral assays subsequent to an acute, systemic injection of vehicle or osanetant.

(G) Number of tail rattles produced during the looming disk assay (see Figure 3C for looming data). SIS-induced tail rattles were attenuated by osanetant.

(H) The effects of acutely administered, systemic osanetant on social interaction (n = 6 mice/condition). Osanetant attenuated SIS-induced reduction in time spent in the social zone.

(I) The effects of osanetant on the acoustic startle assay (n = 8 mice/condition). Osanetant attenuated SIS-induced increased startle responses.

(J and K) Experimental protocol (J) to test whether osanetant also blocked aggression produced by 2 weeks of sexual experience (2 weeks of continuous co-habitation with a female, no isolation). In contrast to the effect of osanetant to attenuate SIS-induced aggression, it had no effect to attenuate sexual experience-induced aggression (K).

(L and M) Experimental protocol (L) to test the effects of osanetant to block shock-induced persistent freezing to the looming disk. All mice were exposed to 4 unsignaled footshocks and tested on the looming disk assay 24 hr later following an acute, systemic administration of vehicle or osanetant. Mice treated with osanetant showed significantly reduced persistent freezing following presentation of the disk compared to vehicle mice (M).

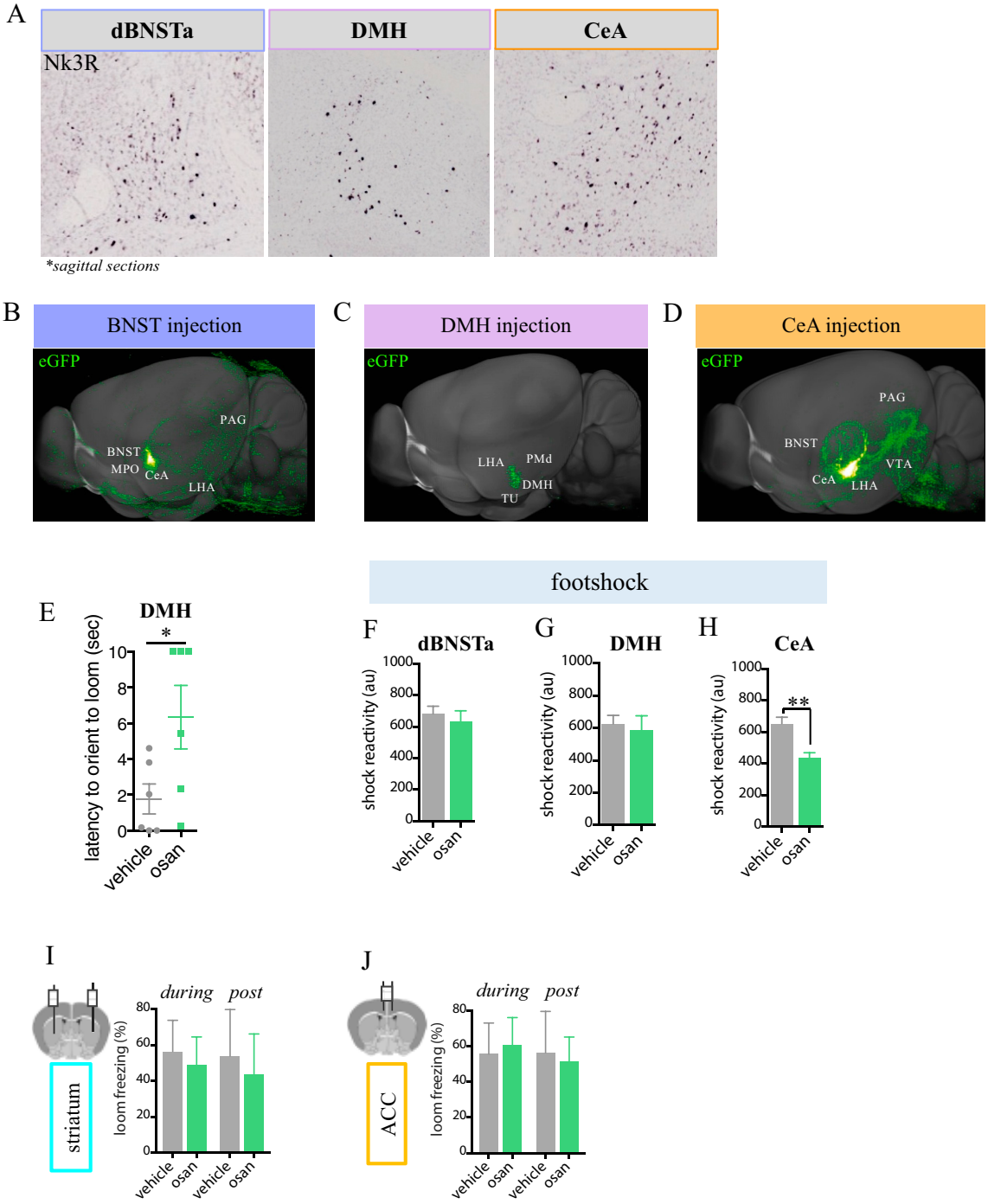

Figure S4. Local Nk3R Antagonism in dBNSTa, DMH, and CeA Blocks Dissociable Effects of SIS on Behavior, Related to Figure 4

(A) Representative sagittal sections illustrating Nk3R expression in the indicated regions (Mouse Brain Atlas, Allen Institute for Brain Science; Exp. 80342167).

(B–D) Representative whole brain 3D images showing injection and projection pattern of a Cre-dependent eGFP viral tracer into the BNST (B), DMH (C), or CeA (D) of Tac2-IRES-Cre mice. (Mouse Connectivity Atlas, Allen Institute for Brain Science; Exp's. 265138021, 300927483, 241279261, respectively). See also Table S2 for projection target regions and density.

(E) The latency to orient to the looming stimulus was increased in SIS mice that had osanetant microinfused into DMH (related to Figure 4F).

(F–H) Reactivity to the footshock in SIS mice with osanetant microinfused into the indicated region. Only CeA osanetant blocked SIS-enhanced shock reactivity. Data are related to Figures 4D, 4G, and 4J.

(I and J) The effect of osanetant microinfusions into the striatum or anterior cingulate cortex (ACC) on freezing behavior in the looming disk assay. No significant effects were observed.

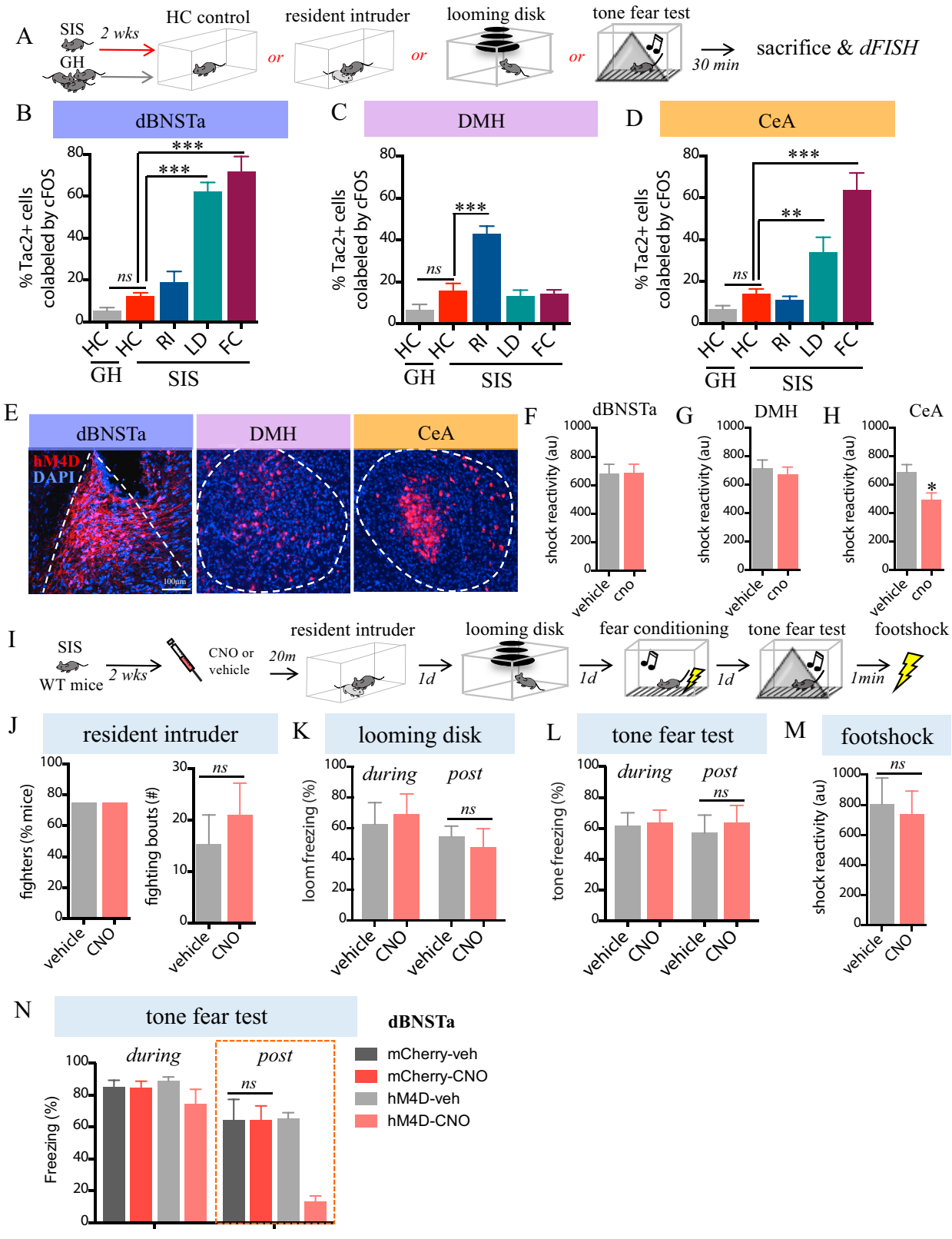

(legend on next page)

Figure S5. Local Chemogenetic Silencing of Tac2^{+} Neurons Reduces the Effects of SIS, Related to Figure 5

(A) Experimental protocol. SIS mice were subjected to the resident intruder assay (RI), the looming disk (LD), or tone fear conditioning and testing (FC). 30 minutes following behavioral testing, mice were sacrificed and brains were collected and processed using dFISH to examine co-expression of Tac2 and Cfos mRNA. SIS and GH mice left in their homecage (HC) served as controls (n = 4 mice/condition; 3-7 sections/mouse).

(B–D) In comparison to SIS HC controls, SIS mice showed a significant increase in cells double labeled for Cfos and Tac2 in the dBNSTa following the LD or FC assay (B), in the DMH following the RI assay (C), and in the CeA following LD and FC (D).

(E) Representative coronal sections of Cre-dependent hM4DREADD-mCherry viral expression in indicated regions of Tac2-IRES-Cre mice.

(F–H) hM4DREADD-driven chemogenetic silencing of Tac2^{+} neurons in CeA (H), but not dBNSTa (F) or DMH (G), attenuated SIS-enhanced shock reactivity. Data related to Figures 5D, 5G, and 5J.

(I) Experimental protocol. WT, naive SIS mice were given an acute, systemic injection of CNO or saline prior to testing on the indicated behavioral assays to control for any non-specific effects of CNO on behavior (n = 8 mice/condition) (see Figure 5).

(J–M) CNO did not significantly alter behavior on any of the assays tested.

(N) Tone fear test for SIS mice injected with AAV2-EF1a-DIO-hM4D-mCherry or AAV2-EF1a-DIO-mCherry control virus in the dBNSTa (n = 6-7 mice per condition). CNO administered to hM4DREADD mice attenuated post-tone persistent freezing, while CNO administered to control mCherry virus-expressing mice produced no significant effects in comparison to vehicle-treated animals.

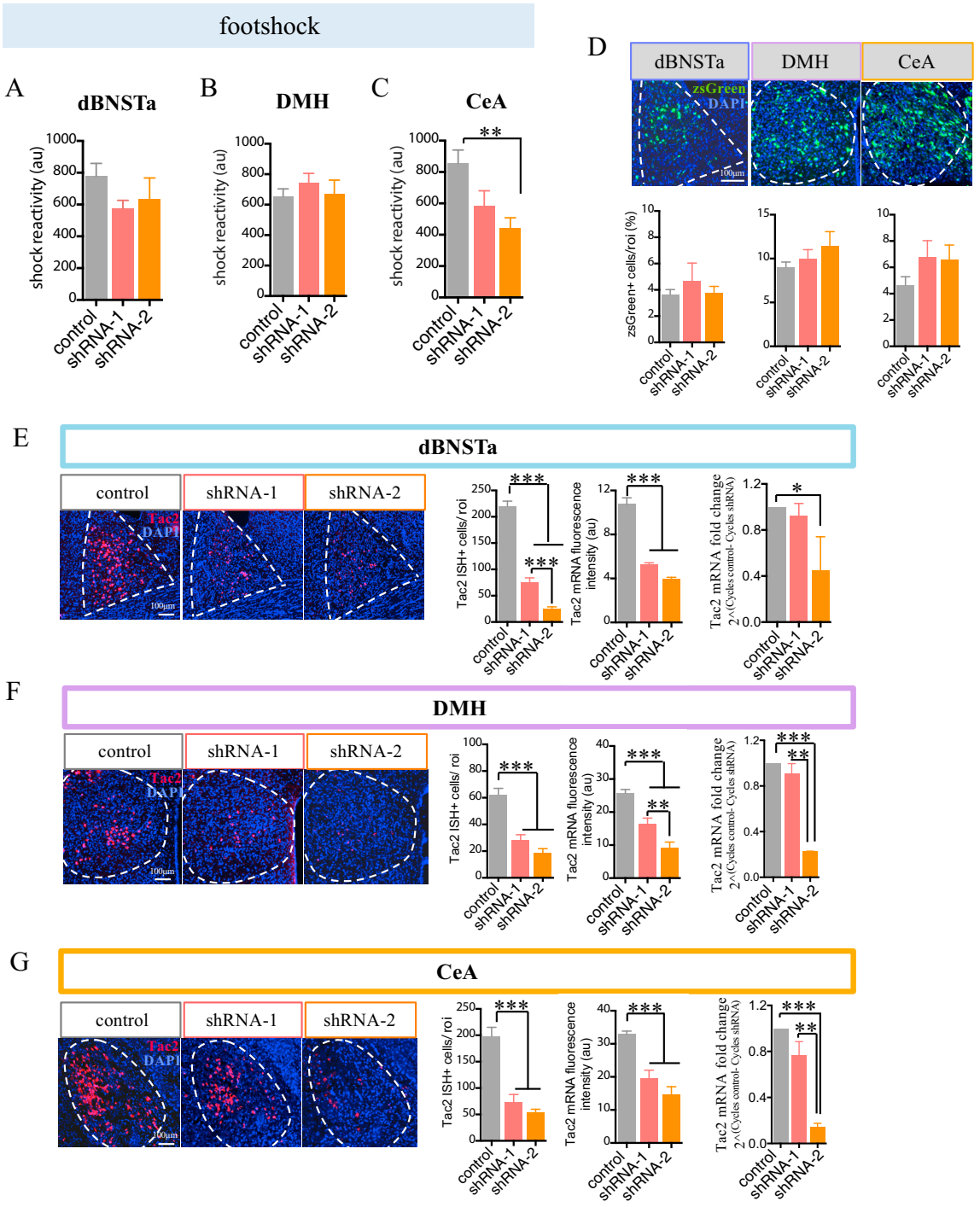

Figure S6. Local Tac2 Knockdown Attenuates the Effects of SIS, Related to Figure 6

(A–C) shRNAi-mediated knockdown of Tac2 in CeA (C), but not dBNST (A) or DMH (B), attenuated SIS-enhanced shock reactivity. Data related to Figures 6D, 6G, and 6J.

(D) Representative coronal sections of shRNA-2-zsGreen viral expression in indicated regions of WT mice (top panels). Lack of any significant difference in the number of zsGreen^{+} cells (lower panels) between Tac2 shRNA virus-injected versus control (luciferase shRNA) virus-injected mice suggests that cell death is not the cause of the Tac2 shRNA phenotypes.

(E–G) Efficacy of Tac2 shRNAs. Following behavior testing, brain sections and tissue taken from shRNA mice were processed for Tac2 mRNA using FISH or qrtPCR to confirm knockdown of Tac2. Representative coronal images, Tac2 mRNA cell counts and intensity, and fold changes in Tac2 mRNA were performed for all animals. Significant decreases in Tac2 mRNA were observed in dBNSTa (E), DMH (F), and CeA (G) (n = 6-7 mice per condition; 4-11 sections/mouse). Note that shRNA-2 produces a stronger knockdown than shRNA-1 in many cases. Dashed white outlines indicate regions within which quantifications were made.

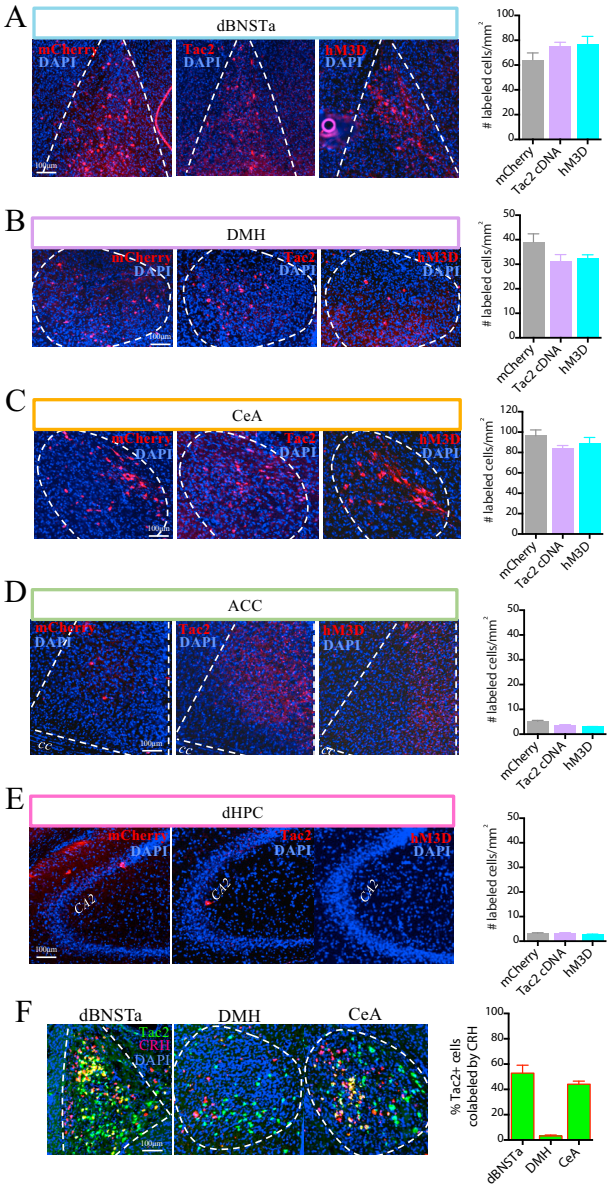

Figure S7. Cre-Dependent CNS Expression from Intravenous Administration of AAV-PHP.B-Encoding GOF Effectors, Related to Figure 7

(A–E) Representative coronal sections to illustrate expression of the control virus mCherry (left panels), Tac2 cDNA-mCherry virus (center panels), or hM3DREADD-mCherry virus (right panels) in the indicated regions of GH mice injected intravenously with the viruses. Quantification of the number of cells expressing each virus per mm^2 is presented alongside each region (right). Number of $mCherry^+$ cells are low in ACC and dHPC because Tac2-Cre expression is low in these regions in GH mice.

"cc," corpus callosum.

(F) SIS mice were sacrificed and brains were processed using dFISH to assess Tac2 and CRH mRNA co-expression (n = 4-5 mice/condition; 4-7 sections/mouse). Tac2 (green) and CRH (red) co-label cells in dBNSTa and CeA, but not DMH. Representative images (left panels) and quantification (right) are shown.